ISSN 1854-6250

APEM journal

Advances in Production Engineering & Management

Volume 10 | Number 3 | September 2015

University of Maribor

Published by PEI
apem-journal.org

Advances in Production Engineering & Management

Identification Statement

APEM journal

ISSN 1854-6250 | Abbreviated key title: **Adv produc engineer manag** | Start year: 2006
ISSN 1855-6531 (on-line)

Published quarterly by **Production Engineering Institute (PEI)**, **University of Maribor**
Smetanova ulica 17, SI – 2000 Maribor, Slovenia, European Union (EU)

Phone: 00386 2 2207522, Fax: 00386 2 2207990
Language of text: English

University of Maribor

APEM homepage: apem-journal.org
University homepage: www.um.si

APEM Editorial

Subscription Rate: 120 EUR for 4 issues (worldwide postage included); 30 EUR for single copies (plus 10 EUR for postage); for details about payment please contact: info@apem-journal.org

Postmaster: Send address changes to info@apem-journal.org

Cover and interior design by Miran Brezocnik
Printed by Tiskarna Koštomaj, Celje, Slovenia

APEM journal is indexed/abstracted in **Scopus** (Elsevier), **Inspec**, **EBSCO** (Academic Search Alumni Edition, Academic Search Complete, Academic Search Elite, Academic Search Premier, Engineering Source, Sales & Marketing Source, TOC Premier), **ProQuest** (CSA Engineering Research Database – Cambridge Scientific Abstracts, Materials Business File, Materials Research Database, Mechanical & Transportation Engineering Abstracts, ProQuest SciTech Collection), and **TEMA** (DOMA). Listed in **Ulrich's** Periodicals Directory and **Cabell's** Directory.

University of Maribor
Production Engineering Institute (PEI)

Advances in Production Engineering & Management

Volume 10 | Number 3 | September 2015 | pp 111–164

Contents

Scope and topics **114**

Characterizations of 304 stainless steel laser cladded with titanium carbide particles **115**
Mahmoud, E.R.I.

An integrated sustainable manufacturing strategy framework using fuzzy analytic network process **125**
Ocampo, L.A.; Clark, E.E.; Tanudtanud, K.V.G.; Ocampo, C.O.V.; Impas Sr., C.G.; Vergara, V.G.; Pastoril, J.; Tordillo, J.A.S.

Effect of a milling cutter diameter on distortion due to the machining of thin wall thin floor components **140**
Sridhar, G.; Ramesh Babu, P.

Experimental and simulation study on the warm deep drawing of AZ31 alloy **153**
Reddy, A.C.S.; Rajesham, S.; Reddy, P.R.

Calendar of events **162**

Notes for contributors **163**

Journal homepage: apem-journal.org

ISSN 1854-6250
ISSN 1855-6531 (on-line)

Scope and topics

Advances in Production Engineering & Management (*APEM journal*) is an interdisciplinary refereed international academic journal published quarterly by the *Production Engineering Institute* at the *University of Maribor*. The main goal of the *APEM journal* is to present original, high quality, theoretical and application-oriented research developments in all areas of production engineering and production management to a broad audience of academics and practitioners. In order to bridge the gap between theory and practice, applications based on advanced theory and case studies are particularly welcome. For theoretical papers, their originality and research contributions are the main factors in the evaluation process. General approaches, formalisms, algorithms or techniques should be illustrated with significant applications that demonstrate their applicability to real-world problems. Although the *APEM journal* main goal is to publish original research papers, review articles and professional papers are occasionally published.

Fields of interest include, but are not limited to:

Additive Manufacturing Processes
Advanced Production Technologies
Artificial Intelligence
Assembly Systems
Automation
Cutting and Forming Processes
Decision Support Systems
Discrete Systems and Methodology
e-Manufacturing
Fuzzy Systems
Human Factor Engineering, Ergonomics
Industrial Engineering
Industrial Processes
Industrial Robotics
Intelligent Systems
Inventory Management
Joining Processes
Knowledge Management
Logistics
Machine Tools
Machining Systems
Manufacturing Systems
Mechanical Engineering
Mechatronics
Metrology
Modelling and Simulation
Numerical Techniques
Operations Research
Operations Planning, Scheduling and Control
Optimisation Techniques
Project Management
Quality Management
Queuing Systems
Risk and Uncertainty
Self-Organizing Systems
Statistical Methods
Supply Chain Management
Virtual Reality

APEM journal
Advances in Production Engineering & Management
Volume 10 | Number 3 | September 2015 | pp 115–124
http://dx.doi.org/10.14743/apem2015.3.196
ISSN 1854-6250
Journal home: apem-journal.org
Original scientific paper

Characterizations of 304 stainless steel laser cladded with titanium carbide particles

Mahmoud, E.R.I.[a,*]

[a]Welding and NDT Laboratory, Manufacturing Technology Department, Central Metallurgical Research and Development Institute (CMRDI), Cairo, Egypt

ABSTRACT

The aim of this paper was to increase the wear resistance of the 304 stainless steel alloy without significant losses of its corrosion resistance. The YAG fiber laser was used to clad it with TiC powder at a fixed processing power of 2800 W and travelling speeds of 4 mm/s, 8 mm/s, and 12 mm/s. The TiC powder with a particle sizes of 3-10 μm were preplaced on a cleaned surface to form a layer of two different thicknesses: 1 mm and 2 mm. The shielding gas that used during and after laser cladding was argon with a flow rate of 15 l/min. Some of the TiC particles were melted and re-solidified as dendrites during the cladding processing. The amount of the dendritic TiC structure was increased by increasing of the travelling speed, and the cohesion of the cladding layer with the substrate was improved for the same reason. At lower travelling speed, cracks were appeared at both the interface and the heat affected zone. The TiC particles were clustered within the top portion of the cladding layer when the preplaced powder was 2 mm. The surface hardness and wear resistance were remarkably improved under all processing conditions, especially at higher travelling speeds. Moreover, the sample treated at a travelling speed of 12 mm/s showed better corrosion resistance than the stainless steel substrate.

ARTICLE INFO

Keywords:
Laser cladding
304 stainless steel alloy
TiC particles
Microhardness
Wear and corrosion resistance

**Corresponding author:*
emahoud@kku.edu.sa
(Mahmoud, E.R.I.)

Article history:
Received 30 December 2014
Revised 19 August 2015
Accepted 24 August 2015

1. Introduction

AISI 304 stainless steel alloy is widely used in many fields, such as oil, nuclear and chemical industries due to its specific properties, i.e. excellent corrosion resistance, good mechanical properties and accepted machinability [1-3]. This type of stainless steels is used as a structural material in hydraulic machinery and in liquid-handling systems [4, 5]. However, at severe environments, where the wear and cavitation attack are the main failure modes, this type of steel cannot be used due to its low surface hardness and wear resistance. Due to the contact between the components and a flowing or vibrating liquid, cavitation erosion represents a common type of degradation of components [6]. Generally, good wear, corrosion and oxidation resistances of different materials can be obtained by tailoring their surface properties. This can be done by depositing some alloys and/or ceramic powders on the material surfaces aiming to produce metal matrix composites (MMCs) on the treated surfaces. This can be produced by laser cladding. The advantages of this technique over the conventional ones (such as arc welding and thermal spraying) include: better coatings with dense microstructure, high wear resistance, low dilution and good metallurgical bonding to substrate [7-9]. Different substrate materials such as steels, aluminum [10, 11] and titanium alloys [12, 13] were cladded by this treatment. Ceramic

powders such as SiC [7], TiC [12, 13], and WC [14] without/or with some materials such as Ni-based alloy [15] were added as cladding materials. TiC is considered a good candidate in this field. This is due to its high thermal stability and high melting point, excellent wear resistance, low coefficient of friction, good resistance to thermal shock, high electrical and thermal conductivities [16]. For these reasons, it is widely used as reinforcement materials in many applications [17-19]. Moreover, the TiC particles have good compatibility with the iron base matrix [20].

Some works have been done to clad the stainless steel alloys with ceramic powder by using laser technique aiming to improve the wear and cavitation erosion resistances [21]. They add hard WC particles to increase the surface hardness which will increase the cavitation erosion resistance [22]. However, these hard WC particles damage the passive film, which is the first defense against any corrosive media [21]. In other studies, the surface hardening of austenitic stainless steel has been achieved by incorporating the hard particles of TiC, SiC, WC and alloying elements [23] in order to form carbides, nitrides [24] and borides [25]. In other studies, element such as Mo [26] was added to improve the pitting and intergranular corrosion resistance and to prevent stress corrosion cracking in acoustic environment. To widen the applications of 304 stainless steel alloy, it is important to improve its wear resistance without losses in its corrosion resistance. In the present study, 304 stainless steel substrate is laser cladded with TiC powder using YAG fiber laser. The effect of travelling speed and the thickness of the preplaced powder on the microstructural features, hardness, wear and corrosion resistance will be studied.

2. Experimental work

Stainless steel (304) specimens with dimensions of 100 mm × 50 mm × 3 mm were used as substrate materials. The specimens were ground using emery papers and cleaned in acetone to remove any dirt, oil, grease and other contaminants before treatment. The TiC powder with a particle size of 3-10 μm were preplaced on the cleaned surface to form a layer of two different thicknesses: 1 mm and 2 mm. The cladding treatments were carried out using YAG fiber laser of 3 kW. To avoid the oxidation during the treatment, argon gas with the flow rate of 15 l/min was used as a shielding gas. The treatments were carried out at fixed processing power of 2800 W, which was considered the optimum power during the preliminary experiments. Three different travelling speeds of 4 mm/s, 8 mm/s, and 12 mm/s were used in this study. The process was conducted at a defocusing distance (D_f) of 65 mm. The laser processed samples were analyzed as described in our work El-Labban et al. [27]. The microstructures of the coated layers were investigated using optical microscope and scanning electron microscope equipped with EDX analyzer. The micro-Vickers hardness in the coated layer cross-section and the substrate were measured with an indentation load of 9.8 N and loading time of 15 s at room temperature. The wear behaviour of the laser cladded zone was evaluated using a pin-on-disk dry sliding wear tester. A stationary sample with a diameter of 2.5 mm was slid against a rotating disk with a rotational speed of 265 rpm for 15 min. The tests were carried out at a fixed load of 2 kg applied to the pin. The differences in average weight before and after the wear test were measured and accounted. Three specimens of each condition were chosen for wear tests. The untreated base metal was selected as the reference material for the wear test. The corrosion behavior of the substrate and the cladding layer were evaluated by the corrosion current density and the corrosion potential obtained from polarization curves in a 3.5 wt.% NaCl solution at room temperature with an IM-6 electrochemical workstation. The scanning potential can be in the range of –1.0 V to +2 V, and the scanning rate was 5 mV/s [27].

3. Results and discussion

3.1 Microstructure analysis

The basic microstructure of the substrate, as shown in Fig. 1, is constituted of equiaxed, twinned austenitic-grain structure, which is the typical microstructure of the 304 austenitic stainless steel alloy. Macro-view of the cross-section of the cladding layer synthesized with laser power

and travelling speed of 2800 W and 12 mm/s, respectively is shown in Fig. 2. The cladding zone appeared as a concaved shape inside the base metal. The used large positive defocusing distance (65 mm) focus the heat into deeper areas, results in this concaved shape. Three zones were appeared in the cross-section of the laser treated area: TiC rich zone, heat affected zone and the substrate, as illustrated in Fig. 2

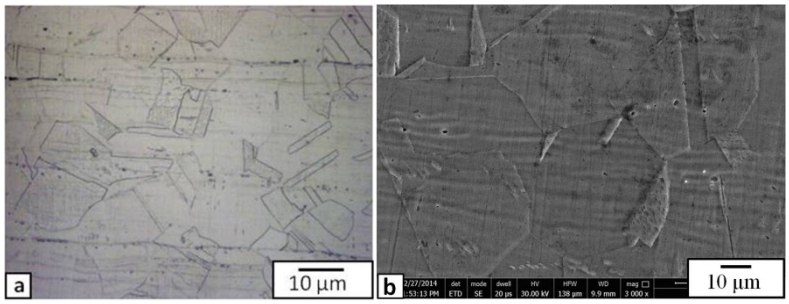

Fig. 1 Microstructure of the 304 stainless steel substrate

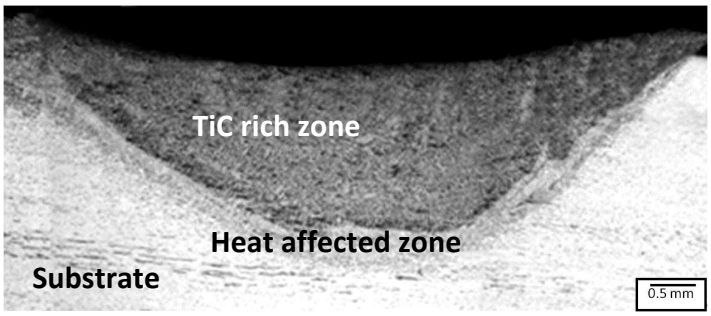

Fig. 2 Macrograph of the laser treated zone at power of 2800 W and travelling speed of 12 mm/s

Fig. 3 and Fig. 4 show the microstructures of the cladded layer fabricated with preplaced TiC powder of 1 mm thick and 4 mm/s travelling speed. Most of the TiC powder were dissolute in the matrix, forming fine dendrites with small arms as shown in Fig. 3(a) and Fig. 3(b). At the lower portion of the cladding layer, many cracks and crack networks were observed which starts from the interface and going upward into the cladding layer as shown in Fig. 3(c) and Fig. 3(d). This is may be due to the lower thermal conductivity of the stainless steel substrate, which may result in keeping of higher temperature for a longer time and reducing the cooling rate, and leads to formation of carbides at the grain boundary of the stainless steel side. This explanation was confirmed with the micrographs shown in Fig. 4. The treated specimen with this slow travelling speed of 4 mm/s had a wide heat affected zone, Fig. 4(a), and their grain boundaries were attacked, Fig. 4(b), due to the formation of carbides at the grain boundaries.

When the travelling speed was increased twice to be 8 mm/s, no micro-cracks were observed in the cladding layer or at the interface as shown in Fig. 5. The cladding layer looks adhered to the substrate and free from the macro-defects. The TiC particles were partially dissolute and appeared as fine long dendrites together with their original shape, especially at the top portion (near the free surface). At the lower portion (near the substrate), the TiC dendrites were shorter and they had random orientation, Fig. 5(b). This is mainly due to the lower heat dissipation to the lower thermal conductivity stainless steel substrate. Moreover, some pores were detected in the cladding layer.

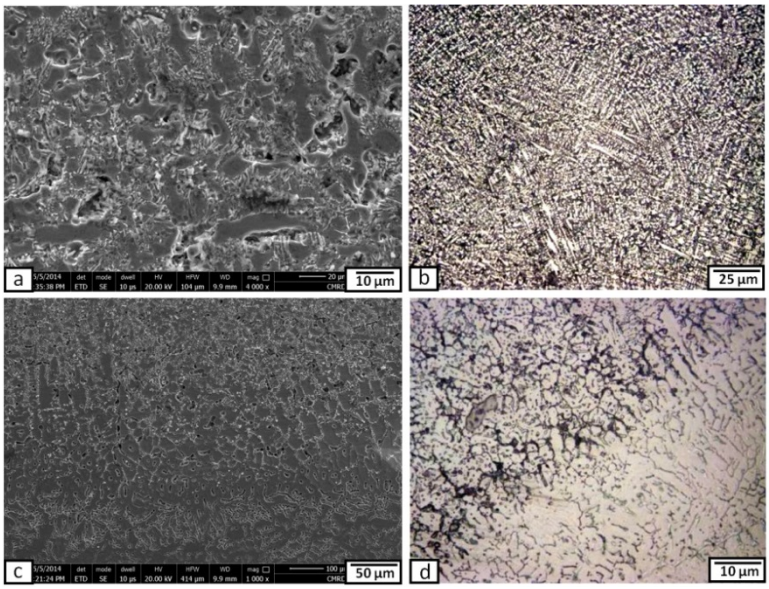

Fig. 3 Micrographs of the different zone at laser treated layer with power of 2800 W and travelling speed of 4 mm/s, when the thickness of preplaced TiC power was 1 mm, where (a) and (b) at the cladding layer, and (c) and (d) at the interface

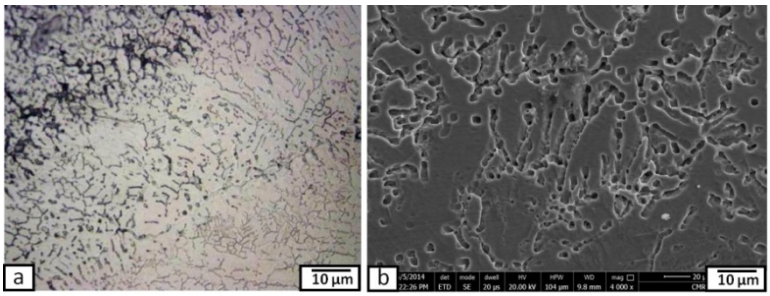

Fig. 4 Micrographs of the heat affected zone of the specimen treated with power of 2800 W and travelling speed of 4 mm/s, when the thickness of preplaced TiC power was 1 mm

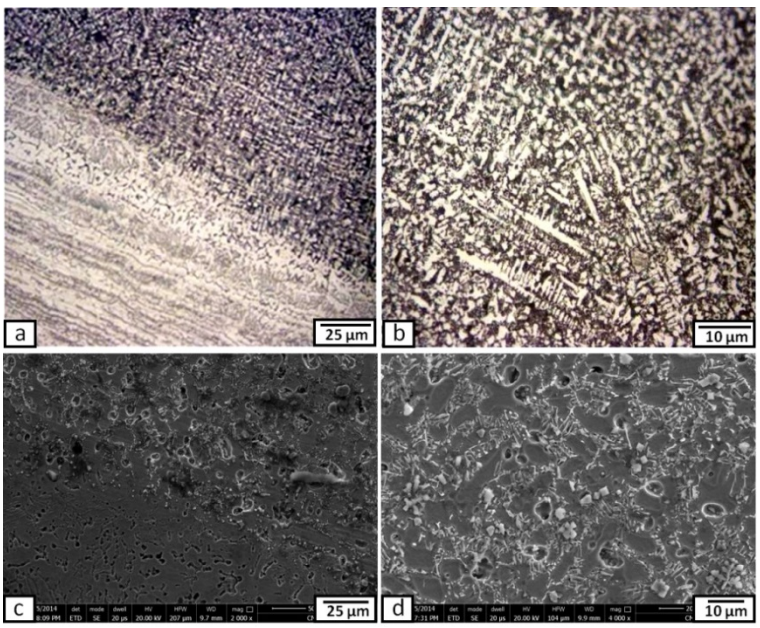

Fig. 5 Micrographs of the different zone at laser treated layer with power of 2800 W and travelling speed of 8 mm/s, when the thickness of preplaced TiC power was 1 mm, where (a) and (c) at the interface, and (b) and (d) at the cladding layer

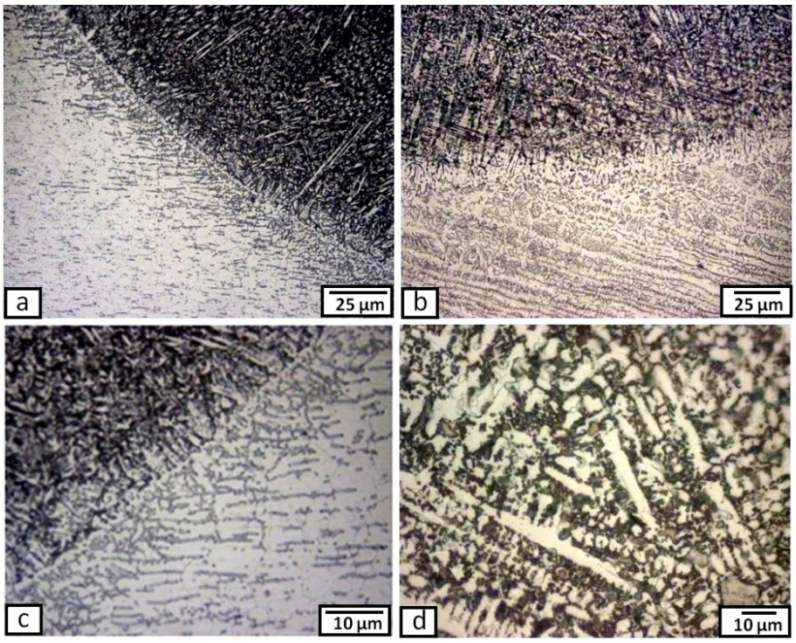

Fig. 6 Micrographs of the different zone at laser treated layer with power of 2800 W and travelling speed of 12 mm/s, when the thickness of preplaced TiC power was 1 mm

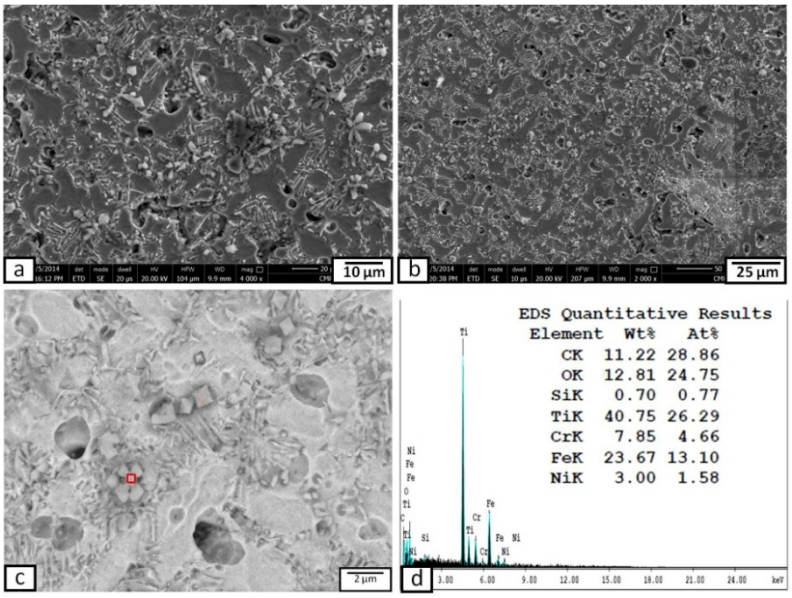

Fig. 7 Micrographs (a - c)of the cladding layer with power of 2800 W and travelling speed of 12 mm/s, when the thickness of preplaced TiC power was 1 mm, and (d) EDX spectra of the elements of red mark in (c)

By increasing the travelling speed to 12 mm/s, the interface between the cladding layer and the substrate stainless steel is adherent, sharp and defect free as shown in Fig 6. The TiC in the cladding layer was distributed homogenously and consisted of fine long dendrites at the top portion and at the lower contour of the cladding layer. This may be due to the relatively fast cooling rate after faster travelling speed. In some areas at the center of the cladding layer, some of the TiC particles appeared as short random oriented dendrites. Moreover, some of these carbides appeared as a rosette shape morphology as shown in Fig. 7.

In severe applications, where the wear is a main failure mode, it is better to increase the thickness of the hard layer deposited on the substrate. For this reason, the thickness of the preplaced TiC powder was increased to be 2 mm. The used processing power and travelling speed were 2800 W and 4 mm/s, respectively. The produced cross-section microstructures were shown in Fig. 8. The cladding layer was consisted of two regions. The TiC powder appeared as

dense clusters of interlocked particles in the upper portion. At these areas, there was almost no stainless steel matrix as shown in Fig. 8(b). The lower portion of the cladding layer was composed of TiC particles with their round shape surrounded by the stainless steel matrix. The heat generated is not enough to melt the thick TiC particles layer. Near the interface, some TiC particles were melted and appeared as dendrites with random orientation or rosette shape as shown in Fig. 9.

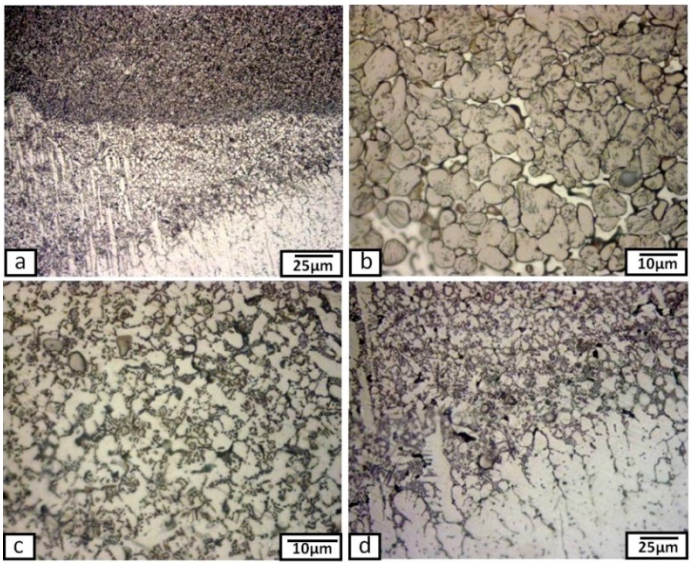

Fig. 8 Micrographs of the different zone at laser treated layer with power of 2800 W and travelling speed of 4 mm/s, when the thickness of preplaced TiC power was 2 mm, where (a) and (d) at the interface, (b) at the top portion of the cladding layer, and (c) at the lower portion of the cladding layer

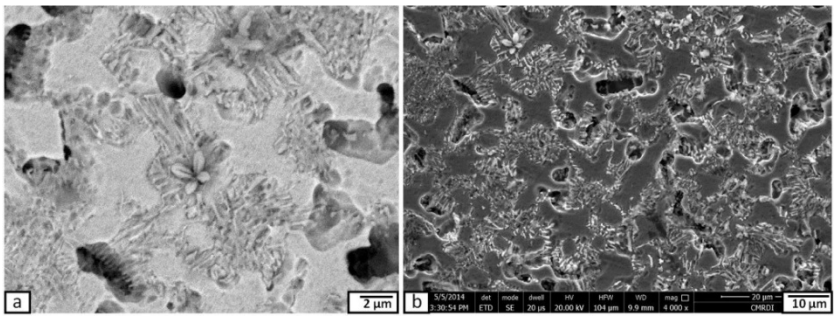

Fig. 9 Micrographs of the cladding layer with power of 2800 W and travelling speed of 4 mm/s, when the thickness of preplaced TiC power was 2 mm

3.2 Surface and subsurface microhardness evaluation

Fig. 10 shows the microhardness distribution through the depth of the laser treated zone obtained at different travelling speeds (4 mm/s, 8 mm/s, 12 mm/s) and preplaced powder thicknesses (1 mm and 2 mm). Generally, the hardness of the cladding layer is much higher (almost three times) than that of the base metal. This is may be due to the hard TiC particles which were distributed homogenously through the cladding layer. The cladding layer which formed with faster travelling speeds show higher hardness that that formed with slower ones. This is due to that the faster travelling speeds yields a finer dendritic TiC, which share in hardness increment. The average hardness values at the surface treated by 12 mm/s travelling speed was about 600 HV.

When the preplaced TiC powder thickness was increased to 2 mm thick, the cladding layer showed ultrahigh hardness values (reached to more than 2000 HV), especially at the top portion of the cladding layer (near the free surface). This is due to the compacted dense hard TiC particles that formed on the top portion of the cladding layer.

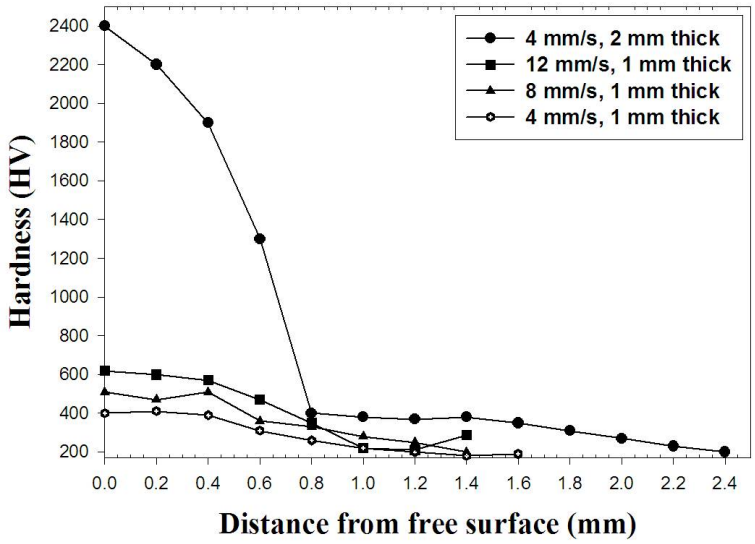

Fig. 10 Microhardness distributions through the laser treated layer cross-sections at different travelling speeds and preplaced powder thicknesses, and fixed power of 2800 W

3.3. Wear and corrosion resistance of the developed surface layer

Fig. 11 shows the variation of wear weight losses of the laser cladding layers using different laser travelling speeds (4 mm/s, 8 mm/s, 12 mm/s) and preplaced powder thicknesses (1 mm and 2 mm) together with the substrate, after subjected to pin-on-disk dry sliding wear test at a fixed load of 2 kg in air at room temperatures. Compared with the substrate, the wear resistance of the laser cladding layer was improved by at least three times. The wear rate was decreased by increasing the travelling speed. This is may be due to the higher hardness achieved at these speeds. On the other hand, the sample that had a preplaced TiC powder of 2 mm, showed exceptional wear resistance (the wear rate was very small, about 0.02 g). This improvement in wear resistance came from the hard, wear resistant, and dense TiC particles which formed at this condition.

Regarding the corrosion resistance evaluation, the sample cladded at travelling speed of 12 mm/s and processing power of 2800 W was chosen due to that it gave the best results regarding the microstructure, hardness and wear resistance. Fig. 12 shows the polarization curves of stainless steel substrate and the cladding layer. The different two branches in each plots represents the anodic (dark one) and cathodic polarization curves. It represents the nature of the reaction at the corrosion potential, e.g., whether the metal is active, passive or active/passive in the corrosion environment. It is well known that when the potential is increased and the current is decreased, the polarization resistance is increased and the material show improved corrosion resistance. From this figure, it is clear that the corrosion current of the cladded layer showed lower values than that of the stainless steel substrate. Also, the corrosion potential of the cladded sample was shifted to more positive than that of the stainless steel substrate. Based on this, the laser cladding of TiC particles on the 304 stainless steel substrate had a positive influence on the corrosion behavior of the coatings. This can be related to the grain refinement of the matrix by the influence of the fast cooling after laser processing. Also, to the good metallurgical bonds of the TiC particles/dendrites with the matrix which give higher chemical stability of the coating. Moreover, the TiC reinforcement acts as obstacles for pitting.

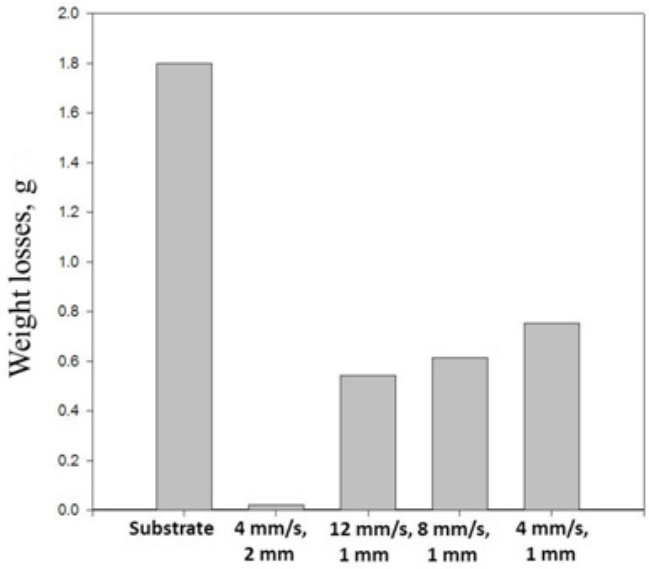

Fig. 11 Wear weight losses of the substrate and specimens treated at different travelling speeds (4 mm/s, 8 mm/s, 12 mm/s) and preplaced powder thicknesses (1 mm and 2 mm), and fixed power of 2800 W

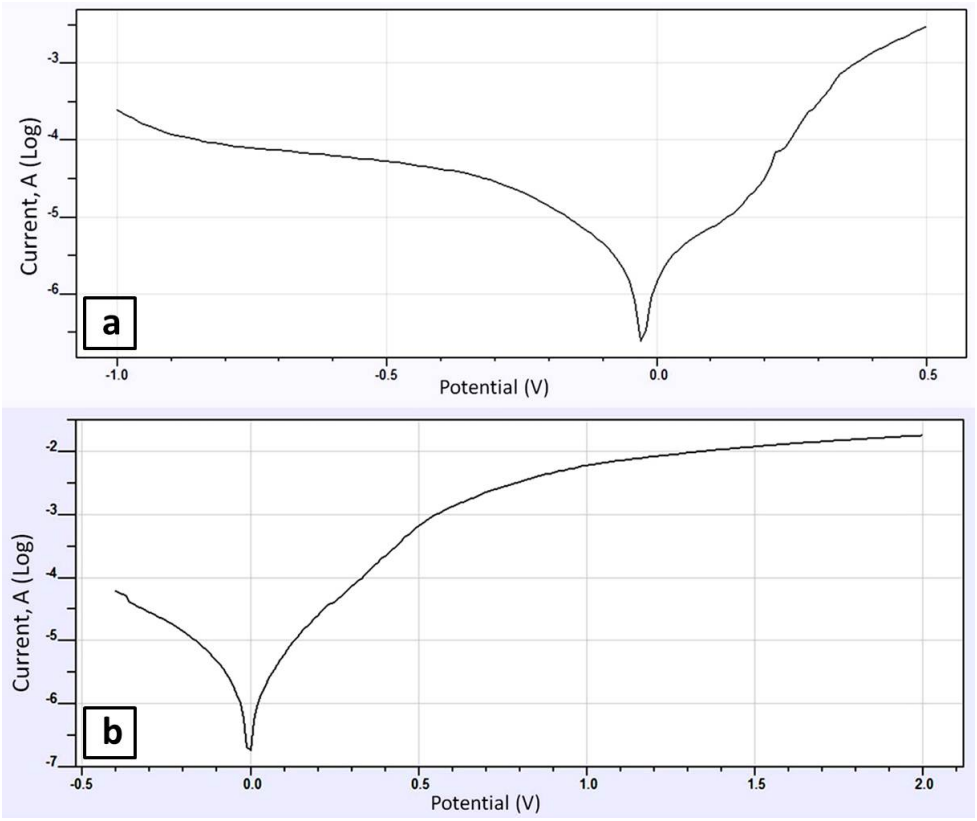

Fig. 12 Polarization curves of the substrate (a), and the cladding layer produced with travelling speed of 12 mm/s and processing power of 2800 W

4. Conclusion

304 stainless steel specimens were YAG fiber laser cladded with TiC powder using processing power of 2800 W and travelling speeds of 4 mm/s, 8 mm/s, and 12 mm/s. The TiC powder with a particle size of 3-10 μm were preplaced on the cleaned surface to form a layer of two different thicknesses: 1 mm and 2 mm. The microstructures of the coated layers and substrate were investigated. The micro-Vickers hardness was measured through the depth of the coated layers cross-section. The wear behaviour of the laser cladded layers was evaluated. The corrosion behavior of the substrate and the cladding layer were evaluated by the corrosion current density and the corrosion potential obtained from polarization curves in a 3.5 wt. % NaCl solution at room temperature. The results of this study lead to the following conclusions:

- Metal matrix composite reinforced with TiC particles was produced in the cladded layer on 304 stainless steel specimens by application of laser cladding treatment at all processing conditions.
- Some of the TiC particles were melted and re-solidified as dendrites during the cladding processing. The amount of the dendritic TiC structure was increased by increasing of the travelling speed.
- The cladding layer produced with higher travelling speed (12 mm/s) was tightly bonded with the substrate without any cracks or any other defects, while that produced at travelling speed of 4 mm/s showed some cracks and crack-networked at the interface and the heat affected zone.
- The TiC particles were clustered in the top portion of the cladding layer when the preplaced powder was 2 mm.
- The hardness of the cladding layer was improved at all processing conditions to be three times at 12 mm/s travelling speed. When the preplaced TiC power was increased to 2 mm, the hardness showed ultrahigh values (more than 2000 HV).
- The wear resistance of the cladding layers was remarkably improved especially at higher travelling speed.
- The corrosion resistance of the cladding layer produced by travelling speed of 12 mm/s was better than that of the stainless steel substrate.

References

[1] Xu, P., Lin, C.X., Zhou, C.Y., Yi, X.P. (2013). Wear and corrosion resistance of laser cladding AISI 304 stainless steel/Al_2O_3 composite coatings, *Surface and Coatings Technology*, Vol. 238, 9-14, doi: 10.1016/j.surfcoat.2013.10.028.

[2] Ul-Hamid, A., Tawancy, H.M., Abbas, N.M. (2012). Failure of weld joints between carbon steel pipe and 304 stainless steel elbows, *Engineering Failure Analysis*, Vol. 12, No. 2, 181-191, doi: 10.1016/j.engfailanal.2004.07.003.

[3] Fissolo, A., Stelmaszyk, J.M., Gourdin, C., Bouin, P., Pérez, G. (2010). Thermal fatigue loading for a type 304-L stainless steel used for pressure water reactor: Investigations on the effect of a nearly perfect biaxial loading, and on the cumulative fatigue life, *Procedia Engineering*, Vol. 2, No. 1, 1595-604, doi: 10.1016/j.proeng.2010.03.172.

[4] Chiu, K.Y., Cheng, F.T., Man, H.C. (2005). Laser cladding of austenitic stainless steel using NiTi strips for resisting cavitation erosion, *Materials Science and Engineering: A*, Vol. 402, No. 1-2, 126-134, doi: 10.1016/j.msea.2005.04.013.

[5] Majumdar, J.D., Chandra, B.R., Manna, I. (2007). Laser composite surfacing of AISI 304 stainless steel with titanium boride for improved wear resistance, *Tribology International*, Vol. 40, No. 1, 146-152, doi: 10.1016/j.triboint.2006.04.006.

[6] Li, S.C. (2000). Cavitation damage in turbines, In: Li, S.C. (ed.), *Cavitation of Hydraulic Machinery*, Imperial College Press, 277-294.

[7] Yang, Y.L., Guo, N., Li, J.F. (2013). Synthesizing, microstructure and microhardness distribution of Ti–Si–C–N/TiCN composite coating on Ti–6Al–4V by laser cladding, *Surface and Coatings Technology*, Vol. 219, 1-7, doi: 10.1016/j.surfcoat.2012.12.038.

[8] Qiu, X.W., Zhang, Y.P., He, L., Liu, C.G. (2013). Microstructure and corrosion resistance of AlCrFeCuCo high entropy alloy, *Journal of Alloys and Compounds*, Vol. 549, 195-199, doi: 10.1016/j.jallcom.2012.09.091.

[9] Guo, C., Zhou, J.S., Chen, J.M., Zhao, J.R., Yu, Y.J., Zhou, H.D. (2010). Improvement of the oxidation and wear resistance of pure Ti by laser cladding at elevated temperature, *Surface and Coatings Technology*, Vol. 205, No. 7, 2142-2151, doi: 10.1016/j.surfcoat.2010.08.125.
[10] Thawari, G., Sundararajan, G., Joshi, S.V. (2003). Laser surface alloying of medium carbon steel with $SiC_{(P)}$, *Thin Solid Films*, Vol. 423, No. 1, 41-53, doi: 10.1016/S0040-6090(02)00974-4.
[11] Liang, G.Y., Wong, T.T., MacAlpine, J.M.K., Su. J.Y. (2000). Study of wear resistance of plasma-sprayed and laser-remelted coatings on aluminium alloy, *Surface and Coatings Technology*, Vol. 127, No. 2-3, 232-237, doi: 10.1016/s0257-8972(00)00551-x.
[12] Sun, R.L., Yang, D.Z., Guo, L.X., Dong, S.L. (2001). Laser cladding of Ti–6Al–4V alloy with TiC and TiC+NiCrBSi powders, *Surface and Coatings Technology*, Vol. 135, No. 2-3, 307-312, doi: 10.1016/S0257-8972(00)01082-3.
[13] Sun, R.L., Mao, J.F., Yang, D.Z. (2002). Microscopic morphology and distribution of TiC phase in laser clad NiCrBSiC–TiC layer on titanium alloy substrate, *Surface and Coatings Technology*, Vol. 155, No. 2-3, 203-207, doi: 10.1016/S0257-8972(02)00006-3.
[14] Mateos, J., Cuetos, J.M., Fernández, E., Vijande, R. (2000). Tribological behaviour of plasma-sprayed WC coatings with and without laser remelting, *Wear*, Vol. 239, No. 2, 274-281, doi: 10.1016/S0043-1648(00)00325-2.
[15] Cheng, F.T., Kwok, C.T., Man, H.C. (2001). Laser surfacing of S31603 stainless steel with engineering ceramics for cavitation erosion resistance, *Surface and Coatings Technology*, Vol. 139, No. 1, 14-24, doi: 10.1016/S0257-8972(00)01103-8.
[16] Mahmoud, E.R.I., El-Labban, H.F. (2014). Laser surface cladding of high C-Cr bearing tool steel with TiC powders, *The IUP Journal of Mechanical Engineering*, Vol. 7, No. 4, 67-79.
[17] Liu, Y.F., Mu, J.S., Xu, X.Y., Yang, S.Z. (2007). Microstructure and dry-sliding wear properties of TiC-reinforced composite coating prepared by plasma-transferred arc weld-surfacing process, *Materials Science and Engineering: A*, Vol. 458, No. 1-2, 366-370, doi: 10.1016/j.msea.2006.12.086.
[18] Dong, Y.J., Wang, H.M. (2009). Microstructure and dry sliding wear resistance of laser clad TiC reinforced Ti–Ni–Si intermetallic composite coating, *Surface and Coatings Technology*, Vol. 204, No. 5, 731-735, doi: 10.1016/j.surfcoat.2009.09.024.
[19] Deng, J.X., Liu, L., Yang, X.F., Liu, J.H., Sun, J.L., Zhao, J.L. (2007). Self-lubrication of Al_2O_3/TiC/CaF_2 ceramic composites in sliding wear tests and in machining processes, *Materials & Design*, Vol. 28, No. 3, 757-764, doi: 10.1016/j.matdes. 2005.12.003.
[20] Moya, J.S., Lopez-Esteban, S., Pecharromán, C. (2007). The challenge of ceramic/metal microcomposites and nanocomposites, *Progress in Materials Science*, Vol. 52, No. 7, 1017-1090, doi: 10.1016/j.pmatsci.2006.09.003.
[21] Lo, K.H., Cheng, F.T., Man, H.C. (2003). Cavitation erosion mechanism of S31600 stainless steel laser surface-modified with unclad WC, *Materials Science and Engineering: A*, Vol. 357, No. 1-2, 168-180, doi: 10.1016/S0921-5093(03)00216-8.
[22] Laroudie, F., Tassin, C., Pons, M. (1995). Hardening of 316L stainless steel by laser surface alloying, *Journal of Materials Science*, Vol. 30, No. 14, 3652-3657, doi: 10.1007/BF00351880.
[23] Guan, K., Wang, Z., Gao, M., Li, X., Zeng, X. (2013). Effects of processing parameters on tensile properties of selective laser melted 304 stainless steel, *Materials & Design*, Vol. 50, 581-586, doi: 10.1016/j.matdes. 2013.03.056.
[24] Viswanathan, A., Sastikumar, D., Rajarajan, P., Kumar, H., Nath, A.K. (2007). Laser irradiation of AISI 316L stainless steel coated with Si_3N_4 and Ti, *Optics & Laser Technology*, Vol. 39, No. 8, 1504-1513, doi: 10.1016/j.optlastec. 2007.01.004.
[25] Zhang, D., Zhang, X. (2005). Laser cladding of stainless steel with Ni-Cr_3C_2 and Ni-WC for improving erosive-corrosive wear performance, *Surface and Coatings Technology*, Vol. 190, No. 2-3, 212-217, doi: 10.1016/j.surfcoat. 2004.03.018.
[26] Majumdar, J.D., Manna, I. (1999). Laser surface alloying of AISI304-stainless steel with molybdenum for improvement in pitting and erosion-corrosion resistance, *Materials Science and Engineering: A*, Vol. 267, No. 1, 50-59, doi: 10.1016/S0921-5093(99)00053-2.
[27] El-Labban, H.F., Mahmoud, E.R.I., Al-Wadai, H. (2014). Laser cladding of Ti-6Al-4V alloy with vanadium carbide particles, *Advances in Production Engineering & Management*, Vol. 9, No. 4, 159-167, doi: 10.14743/apem 2014.4.184.

APEM journal
Advances in Production Engineering & Management
Volume 10 | Number 3 | September 2015 | pp 125–139
http://dx.doi.org/10.14743/apem2015.3.197
ISSN 1854-6250
Journal home: apem-journal.org
Original scientific paper

An integrated sustainable manufacturing strategy framework using fuzzy analytic network process

Ocampo, L.A.[a,*], **Clark, E.E.**[b], **Tanudtanud, K.V.G.**[c], **Ocampo, C.O.V.**[d], **Impas Sr., C.G.**[a], **Vergara, V.G.**[a], **Pastoril, J.**[a], **Tordillo, J.A.S.**[a]

[a]University of San Carlos, Department of Mechanical Engineering, Cebu City, Cebu, Philippines
[b]De La Salle University, Department of Industrial Engineering, 2401 Taft Avenue, Manila, Philippines
[c]International Society for Business Innovation & Technology Management (ISBITM), Radium St., Manila, Philippines
[d]University of San Carlos, Department of Industrial Engineering, Cebu City, Cebu, Philippines

ABSTRACT

This paper adopts a fuzzy analytic network process approach for developing a sustainable manufacturing strategy under the influence of stakeholders' interests. Frameworks developed in literature tend to structure manufacturing strategy in such a way that addresses market needs and expectations. As the move towards sustainability becomes highly pronounced, literature in domain manufacturing is developing approaches and initiatives that explore different facets of sustainability. However as this impetus becomes increasingly famous, manufacturing firms are faced with the challenge of integrating sustainability with the classical function of manufacturing, which is to support firms' competitive advantages. Thus, an inclusive approach would constitute a manufacturing strategy that would support not only sustainability but enhance the competitive strategy of a firm. In order to integrate these two objectives it is necessary to take into consideration the different stakeholders' interests as significant drivers towards sustainability. This work explores the significance of these interests when developing a manufacturing strategy using the proposed approach. In the proposed method, an analytic network process handles the complexity of the decision framework, and judgment elicitation during pairwise comparisons is described using linguistic variables with equivalent triangular fuzzy numbers. The proposed approach is useful when handling complexity and uncertainty especially in group decision-making. The content of the sustainable manufacturing strategy using a fuzzy analytic process is presented in this paper.

ARTICLE INFO

Keywords:
Manufacturing strategy
Sustainability
Uncertainty
Analytic network process
Fuzzy set theory

**Corresponding author:*
don_leafriser@yahoo.com
(Ocampo, Lanndon A.)

Article history:
Received 20 May 2015
Revised 12 August 2015
Accepted 19 August 2015

1. Introduction

The classical model of Skinner [1] and Wheelwright [2] on manufacturing strategy was highly motivated by market behavior and market requirements. Resulting from buying experiences, dynamic needs, etc., the market creates a priority set of the four widely accepted competitive priorities which are cost, quality, dependability and flexibility [2-4]. This prioritization process of the market motivates the priority set of competitive priorities of a business unit which eventually influences the manufacturing function. When manufacturing decisions are consistent over nine decision categories, manufacturing creates capabilities which must be positioned in line with the competitive priorities set up by the business unit. This network of influences seems to function only when the market is solely the focal point of interest. However, this network fails to

address the conditions that demand simultaneous considerations of several stakeholders. The best example of these conditions is sustainability-related issues. Thus, an update of this network becomes necessary to address the complex interests of various stakeholders.

An emerging body of literature claims that the role of stakeholders in the sustainability efforts of firms is arguably significant [5-7]. Aside from exerting pressures on manufacturing firms which is the general claim [8], stakeholders could assist firms in deciding which environmental and social initiatives to adopt because stakeholders have already established some forms of perspectives, experiences and resources vital in addressing sustainability issues. Creating initiatives that enhance close relations with employees and suppliers advances the capability of firms in integrating environmental aspects into key organizational processes. With the emerging issues on sustainability encountered by manufacturing firms, manufacturing organizations must proactively create value through investment in customers, suppliers, employees, processes, technology and innovation [9]. Models developed by previous literature lack quantitative integration of manufacturing strategy and sustainable manufacturing into a framework that addresses both sustainability and competitiveness.

This paper aims to develop the content of a sustainable manufacturing strategy with the influence of different stakeholders' interests. This is significant as it provides possible direction for manufacturing industry on the policy options that must be made in order to address both competitiveness and sustainability of manufacturing. Due to the multi-criteria nature of the decision problem under vague decisions which are brought about by the subjective nature of most of the criteria, a fuzzy analytic network process is thus used. This approach was also used in identifying the structural decisions of sustainable manufacturing strategy under the relevance of firm sizes [10] and of the strategic responses of firms [11]. Fuzzy set theory handles the uncertainty of decision-making [12] while analytic network process is a multi-criteria decision making tool which is used to handle complex decision-making [13]. The use of analytic network process and its special case, the analytic hierarchy process, in strategy and sustainability research is rich in literature, e.g. Ocampo and Clark [14], Ocampo [15], Pan et al. [16]. The contribution of this work lies in developing a comprehensive framework in identifying specific decisions that comprise a sustainable manufacturing strategy with the influence of stakeholders' interests.

2. Literature review

2.1 Manufacturing strategy

Definitions of manufacturing strategy presented by previous studies can be summarized into few unifying concepts. First, manufacturing strategy represents a pattern of coordinated and consistent decisions over a relatively narrow area [17]. Second, manufacturing strategy determines the capabilities of the manufacturing function and provides its competitive advantage [18]. Lastly, manufacturing strategy is consistent with the objectives of the business strategy [17-19]. Inspired largely by the work of Skinner [1], subsequent works agreed that manufacturing function involves a number of decision categories which are shown in Table 1.

Depending on the decisions made within these categories, manufacturing strategy develops a set of capabilities [21]. Four competitive priorities were widely known in literature: cost, quality, dependability and flexibility [2, 3].

Table 1 Manufacturing decision categories

Manufacturing decision categories	Source	Policy areas [2, 20]
Process technology	[2, 3, 20]	Process choice, technology, integration
Facilities	[1-3, 20]	Size, location, focus
Capacity	[2, 3, 20]	Amount, timing, type
Vertical integration	[2, 3, 20]	Direction, extent, balance
Organization	[1, 3, 20]	Structure, reporting levels, support groups
Manufacturing planning and control	[1, 2, 20]	System design, decision support, systems integration
Quality	[2, 3, 20]	Defect prevention, monitoring, intervention
New product introduction	[1, 3, 20]	Rate of innovation, product design, industrialization
Human resources	[1-3]	Skill level, pay, security

Competing on cost requires a manufacturing strategy that minimizes the inefficiencies of manufacturing operations so that products are offered at low costs. This is addressed by labor, materials, capital returns, inventory turnover and unit costs [3]. Manufacturing strategy that emphasizes quality as the dominant capability requires higher quality in standard product or one that offers broader features or performance characteristics compared to other competitors with similar products. Measurement could be percent defectives, frequency field failure, cost of quality and mean time between failures [3]. Dependability involves a manufacturing system that is able to do work as specified, delivered on time and the firm makes sure that its resources are ready so that any failures are corrected immediately. It could be achieved by dealing on product mix flexibility, volume flexibility and lead time for new products [3]. Measurement indicators could be percentage of on-time shipments, average delay and expediting response time [3]. A comprehensive discussion of these four capabilities was outlined by Ward et al. [22].

Note that the competitive strategy reinforced by the manufacturing strategy must support the competitive advantage defined by the business strategy as depicted by Skinner's [1] hierarchical framework. Moreover, aside from maintaining this competitive advantage, the strategy adopted must create and maintain the manufacturing competitive position in the market. Different manufacturing firms emphasize each of the four competitive capabilities in varying degrees [2]. To summarize, manufacturing strategy is derived from business and corporate strategies [1] which are largely driven by the market. Market establishes the requirements of the business unit and consequently identifies the set of competitive priorities. Manufacturing strategy provides the necessary policy to support the strategy of the business while at the same time creates capabilities in the long run. This framework generally addresses competitiveness of the business unit with limited information on how this works when sustainability is eventually placed into the context. One challenging issue that needs to be resolved in the framework is the presence of stakeholders' interests that must be considered when confronting sustainability agenda.

2.2 Sustainable manufacturing

While other economic sectors share responsibilities in addressing sustainability, manufacturing sector is undoubtedly an important piece of the puzzle [23]. With expected five-fold increase in GDP per capita over the next fifty years, a corresponding ten-fold increase in total impact in energy consumption, material usage and wastes generation is expected [24]. Hassine et al. [25] pointed out that the energy consumption of manufacturing industries account for 30 % of the global energy demand and 36 % of the global carbon dioxide emissions. This consumption implies adverse environmental impact and degradation of natural resources [25]. Being the leading employment sector and main contributor to the GDP, the manufacturing sector serves as the "backbone" to the well-being of nations and societies [24]. With this, sustainable manufacturing, as an approach, has emerged and is defined by the U.S. Department of Commerce as "the creation of manufactured products that use processes that minimize negative environmental impacts, conserve energy and natural resources, are safe for employees, communities and consumers and are economically sound" [26]. Sustainable manufacturing gained overwhelming interests both in industry and academia and inspired leading developed economies to design responsive policy platforms [27]. Nevertheless, this approach gained global momentum [28].

A concise framework on sustainability in general and on sustainable manufacturing in particular is the triple-bottom line approach [29, 30] which was introduced by Elkington [31]. This approach maintains that sustainable manufacturing is achieved by simultaneously considering environmental stewardship, economic growth, and social well-being [26]. This framework has been adopted by various operations management researches [32-35]. While this sounds impressive, it does not provide clear direction on the competitive function of manufacturing as described by Skinner's [1] framework. Conceptual frameworks are on sustainable manufacturing based on the TBL approach. These could be summarized as follows: (1) sustainability is further achieved through collaboration in the supply chain [36, 37], (2) a comprehensive approach to sustainability is through the life-cycle approach [38, 39], and (3) different stakeholders have significant roles in sustainability transformation [40, 41].

2.3 Stakeholders' interests

Recent studies have placed high regard on the role of stakeholders in forging sustainability of manufacturing organizations, e.g. [42-44]. Stakeholders comprise those who are influenced, either directly or indirectly, by the actions carried out by the firm [9]. These include employees, suppliers, customers, industry associations, universities, consultants, governments, community organizations, and the media [44]. Pham and Thomas [9] argue that traditional organizations tend to focus only on a handful, limited number of stakeholders with special attention to shareholders such as board of directors and investors. Griffiths and Petrick [42] contend that such approach fails to develop stakeholder integration for firms. A widely accepted notion is that when stakeholders are managed well, they are capable in offering invaluable assistance and resources beyond simply exerting pressures on firms [45, 46]. For instance, customers can possibly exert pressure on suppliers to establish environmental programs as a precondition to supply [7]. On the other hand, employees can provide recommendations for advancing firm's responsibility to the community by pointing out inputs related to the current socio-economic conditions of the local community. Suppliers play a critical role in providing insights which are associated to technology, materials and processes that could be helpful in strengthening firm's environmental efforts [47, 48]. Harrison et al. [49] claim that manufacturing firms are likely to build trusting relations across several stakeholders when firms integrate them in their key decision-making processes. Having stronger relations with stakeholders, necessary insights for deciding how to allocate limited resources in order to satisfy stakeholders are certainly gained.

3. Methodology

3.1 Fuzzy set theory

Fuzzy set theory was developed by Zadeh [50] as a mathematical approach of handling imprecision and vagueness in decision-making. A fuzzy number can be represented by a fuzzy set $F = \{(x, u_F(x)), x \in \mathbb{R}\}$ where $x \in \mathbb{R}$ and $u_F(x) \rightarrow [0,1]$. The binary set [0, 1] is a crisp set and any value that is represented between 0 and 1 indicates partial acceptance. Various types of fuzzy numbers emerge in literature but the widely used one is the triangular fuzzy number (TFN) [51, 52]. TFN can be defined as a triplet $A = (l, m, u)$ and the membership function $\mu_{\widetilde{M}}(x)$ can be defined as

$$\mu_A(x) = \begin{cases} 0 & x < l \\ (x-l)/(m-l) & l \le x \le m \\ (u-l)/(u-m) & m \le x \le u \\ 0 & x > u \end{cases} \quad (1)$$

and the representation of a TFN is

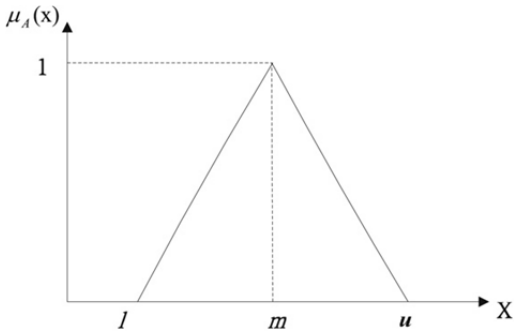

Fig. 1 A TFN A = (l, m, u) [10]

Suppose two TFNs $\tilde{A}$ and $\tilde{B}$ are defined by the triplet (a_1, a_2, a_3) and (b_1, b_2, b_3), respectively. The basic operations of these two TFNs are as follows:

$$\tilde{A} + \tilde{B} = (a_1, a_2, a_3) + (b_1, b_2, b_3) = (a_1 + b_1, a_2 + b_2, a_3 + b_3) \quad (2)$$

$$\tilde{A} - \tilde{B} = (a_1, a_2, a_3) - (b_1, b_2, b_3) = (a_1 - b_1, a_2 - b_2, a_3 - b_3) \quad (3)$$

$$\tilde{A} \otimes \tilde{B} = (a_1, a_2, a_3) \times (b_1, b_2, b_3) = (a_1 b_1, a_2 b_2, a_3 b_3) \quad (4)$$

$$\tilde{A} \div \tilde{B} = (a_1, a_2, a_3) \div (b_1, b_2, b_3) = (a_1 \,/\, b_3, a_2 \,/\, b_2, a_3 \,/\, b_1) \quad (5)$$

FST enhances the capability of MCDM methods in handling complex and imprecise judgments [10]. Most evaluators could hardly elicit exact numerical values to represent opinions based on human judgment [52]. More realistic evaluations use linguistic variables to represent judgment rather than numerical values [53]. Linguistic variable represents linguistic values with form of phrases or sentences in a natural language [54]. Expressing judgment in linguistic variables is a useful method in dealing with situations that are described in quantitative expressions [53]. The integration of fuzzy set theory in the context of AHP/ANP draws several techniques. Refer to the work of Promentilla et al. [51], Wang et al. [55], Ocampo and Clark [56] for a review on these techniques. The approach adopted in this study shares similarity with the works of Tseng [12, 52] which transform TFNs into crisp values before raising the pairwise comparisons matrices to large powers. This method has been used because of the simplicity of the approach and the validity of previous works that embarked on it. Tseng [52] argued that any fuzzy aggregation method must contain defuzzification method. An algorithm in determining the crisp values was proposed by Opricovic and Tzeng [57]. The linguistic variables are presented in Table 2 with equivalent TFNs adopted from Tseng et al. [58].

Table 2 Linguistic variables adopted from Tseng et al. [58]

Linguistic scale	Code	Triangular fuzzy scale	Triangular fuzzy reciprocal scale
Just equal		(1,1,1)	(1,1,1)
Equal importance	EQ	(1/2,1,3/2)	(2/3,1,2)
Moderate importance	MO	(5/2,3,7/2)	(2/7,1/3,2/5)
Strong importance	ST	(9/2,5,11/2)	(2/11,1/5,2/9)
Demonstrated importance	DE	(13/2,7,15/2)	(2/15,1/7,2/13)
Extreme importance	EX	(17/2,9,9)	(1/9,1/9,2/17)

Let $\widetilde{w}_{ij}^{k} = \left(a_{1ij}^{k}, a_{2ij}^{k}, a_{3ij}^{k}\right)$ be the influence of ith criteria on jth criteria assessed by the kth evaluator. The defuzzification process proposed by Opricovic and Tzeng [57] is as follows:

Step 1: Normalization

$$xa_{1ij}^{k} = \frac{a_{1ij}^{k} - min\, a_{1ij}^{k}}{\Delta_{min}^{max}} \quad (6)$$

$$xa_{2ij}^{k} = \frac{a_{2ij}^{k} - min\, a_{1ij}^{k}}{\Delta_{min}^{max}} \quad (7)$$

$$xa_{3ij}^{k} = \frac{a_{3ij}^{k} - min\, a_{1ij}^{k}}{\Delta_{min}^{max}} \quad (8)$$

where

$$\Delta_{min}^{max} = max\, a_{3ij}^{k} - min\, a_{1ij}^{k}.$$

Step 2: Computation of left ls and right rs normalized values

$$xls_{ij}^{k} = \frac{xa_{2ij}^{k}}{1 + xa_{2ij}^{k} - xa_{1ij}^{k}} \quad (9)$$

$$xrs_{ij}^{k} = \frac{xa_{3ij}^{k}}{1 + xa_{3ij}^{k} - xa_{2ij}^{k}} \tag{10}$$

Step 3: Computation of total normalized crisp value

$$x_{ij}^{k} = \frac{xls_{ij}^{k}\left(1 - xls_{ij}^{k}\right) + xrs_{ij}^{k} xrs_{ij}^{k}}{1 - xls_{ij}^{k} + xrs_{ij}^{k}} \tag{11}$$

Step 4: Computation of crisp values

$$w_{ij}^{k} = min\, a_{1ij}^{k} + x_{ij}^{k}\Delta_{min}^{max} \tag{12}$$

3.2 Analytic network process

ANP is the general theory of analysing complex decision problems where analytic hierarchy process (AHP) is a special case. Local priorities in ANP are obtained similar to how local priorities in AHP are computed; that is, by performing paired comparisons. In ANP, the decision problem is structured as a network of constructs that describes dependence relations of one component on another component. The advantage of using ANP in a wide array of decision problems is in capturing both qualitative and quantitative criteria in a model that attempts to resemble reality. The input of local priorities depends on the presence and type of dependence relations described in the network. The eigenvector method, as described in the theory of Oskar Perron which was discussed by Saaty [59], is referred to as the exact way of computing relative local priorities of these elements. Saaty [60] proposed an eigenvalue problem to obtain the desired ratio-scale priority vector (or weights) *w* of *n* elements:

$$Aw = \lambda_{max} w \tag{13}$$

where A is the positive reciprocal pairwise comparisons matrix, λ_{max} is the maximum (or principal) eigenvalue of matrix A. For consistent judgment, $\lambda_{max} = n$, otherwise, $\lambda_{max} > n$. The measure of judgment consistency is measured using the Consistency Index (CI) and Consistency Ratio (CR). The Consistency Index (CI) is a measure of the degree of consistency and is represented by

$$CI = \frac{\lambda_{max} - n}{n - 1} \tag{14}$$

The consistency ratio (CR) is computed as

$$CR = \frac{CI}{RI} \tag{15}$$

where RI is the mean random consistency index. $CR \leq 0.10$ is an acceptable degree of inconsistency. Decision-makers would be asked to reconsider the paired comparisons in case of $CR > 0.10$.

Global priority ratio scales or priorities can be computed based on the synthesizing principle of the supermatrix [51]. By raising the matrix to large powers, the transmission of influence along all possible paths in the network is captured in the process [13]. The convergence of initial priorities (stochastic matrix) to an equilibrium value in the limit supermatrix provides a set of meaningful synthesized priorities from the underlying decision network [51]. Saaty [13] assured that as long as the supermatrix representation is a primitive irreducible matrix in a strongly connected digraph, the initial supermatrix will eventually converge to a limit supermatrix. The numerical approach of solving the limit supermatrix denoted by L is by normalizing columns and then raising the supermatrix to $p = 2k + 1$ power where k is an arbitrary large number.

$$\lim_{p\to\infty}\left(\frac{S}{\lambda_{max}}\right)^{p} = \lim_{p\to\infty}(\bar{S})^{p} = L \tag{16}$$

Each column of the limit supermatrix is a unique positive column eigenvector associated with the principal eigenvalue λ_{max} [51]. This resembles the priorities of the limit supermatrix and can be used to measure the overall relative dominance of one element over another element in a network [51].

3.3 Procedure

To summarize, the research procedure implemented in this paper is as follows:

1. Perform pairwise comparisons based from the decision network motivated from literature. The generic question that is asked in doing pairwise comparison is "Given a control element, a component (element) of a given network, and given a pair of component (or element), how much more does a given member of the pair dominate other member of the pair with respect to a control element?" [51]. Instead of using the Saaty's fundamental scale, comparisons are made using linguistic scales as shown in Table 2.
2. Transform linguistic variables into corresponding TFNs in Table 2. Using Eq. 6 through Eq. 12, compute corresponding crisp values of the TFNs.
3. Compute local priority vectors, *CI* and *CR* values of pairwise comparisons matrices using Eq. 13 through Eq. 15. If $CR > 0.10$, decision-makers should be asked to reconsider judgments in paired comparisons.
4. Aggregate the pairwise comparisons matrices of decision-makers using Eq. 17. After constructing aggregated pairwise comparisons matrices, compute local priority vectors of these matrices using Eq. 13.

$$\overline{w}_{ij} = \left(\prod_{k} w_{ij}^{k}\right)^{1/k} \tag{17}$$

5. Construct an initial supermatrix from the decision network developed in step 1. Then, populate this initial supermatrix with the local priority vectors obtained in step 4. Normalize the columns of the initial supermatrix in order to attain a stochastic matrix. Then raise the stochastic matrix to large powers Eq. 16 to compute for the final priority vector.

4. Decision model

Following the literature review in Section 2, the decision model can be described into two parts. The first part presents the hierarchical structure of decision categories, policy areas and policy options. This shows that each decision category is composed of policy areas and each policy area has policy options or choices. This part is largely influenced by the second part of the model. The second part illustrates the relationships of stakeholders' interests, competitive priorities and strategic responses. Stakeholders' interests dominate competitive priorities which is vital in sustainability. Instead of the market exclusively setting up the competitive priorities consistent with the former arguments of Wheelwright [2], the model holistically considers the interests of different stakeholders in determining competitive priorities. These priorities influence the strategic responses of firms toward sustainability. In effect, these responses influence the decisions which would eventually comprise the sustainable manufacturing strategy. Fig. 2 shows the decision model developed in this work.

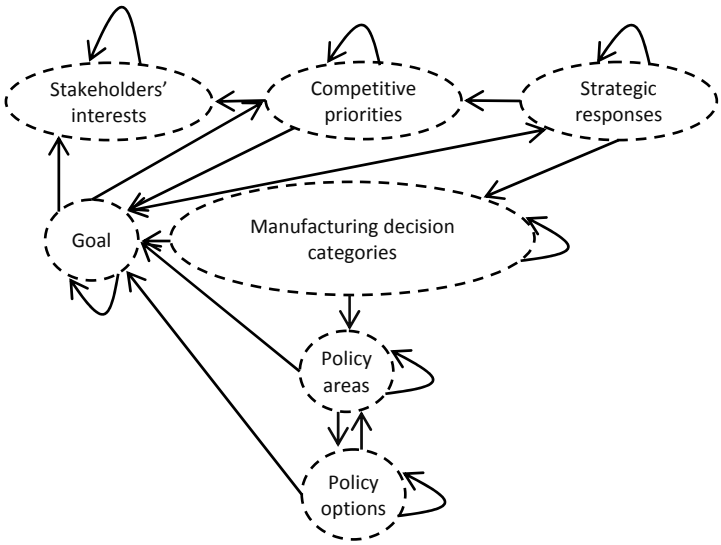

Fig. 1 Proposed decision model

The decision model in Fig. 2 has six components which are composed of the goal, stakeholders' interests, competitive priorities, strategic responses, manufacturing strategy decision categories, policy areas and policy options. These components are linked together in a network of dependence relations. Each component of the model comprises respective decision elements. The goal component contains a single element which is to develop SMS. Stakeholders' interests have two sub-components: stakeholders' component which has eight decision elements and stakeholders' interests' component with 28 children elements. Competitive priorities have four elements as discussed in the previous section. Strategic responses have three elements which are stakeholder-oriented, market-oriented and sustainability-oriented. Manufacturing decision categories component has nine elements and each element has its own set of policy areas as described in Table 1. Furthermore, each policy contains policy options which a manufacturing firm could deliberately choose from. The objective of this work is to analytically choose a particular set of options that comprise SMS which best addresses the goal resulting from the interrelationships of the components and elements described in Fig. 2. In order to facilitate easier computations, a comprehensive coding system is shown in Table 3 to represent each element in the decision model. The coding system is so structured to facilitate remembering of elements associated with their parent element.

Table 3 Coding system of the stakeholder-motivated competitive priority decision model

Decision components	Decision elements	Code	Decision components	Decision elements	Code
Goal	develop sustainable manufacturing strategy	A	Policy options	job shop	C111
Stakeholders	government	H1		batch	C112
	suppliers	H2		continuous	C113
	shareholders	H3		project	C114
	business customers	H4		robotics	C121
	consumers	H5		flexible manufacturing system	C122
	community	H6		computer-aided manufacturing	C123
	employees	H7		cellular	C131
	competitors	H8		process	C132
Stakeholders' sustainability interests	government's increased taxes	H11		product	C133
	government's environmental protection	H12		one big plant	C211
	government's health & safety	H13		several smaller ones	C212
	suppliers' compliance with international standards	H21		close to market	C221
	suppliers' quality	H22		close to supplier	C222
	suppliers' cost	H23		close to technology	C223
	suppliers' delivery	H24		close to competitor	C224

Table 3 Coding system of the stakeholder-motivated competitive priority decision model (continuation)

	shareholders' profitability	H31	close to source of raw materials	C225
	shareholders' environmental equity	H32	product groups	C231
	shareholders' social equity	H33	process types	C232
	business customers' quality	H41	life cycle stages	C233
	business customers' cost	H42	fixed units per period	C311
	business customers' delivery	H43	based on inputs	C312
	business customers' international certifications	H44	based on outputs	C313
	consumers' quality	H51	leading	C321
	consumers' cost	H52	chasing	C322
	consumers' delivery	H53	following	C323
	community's environmental effect	H61	potential	C331
	community's employment	H62	immediate	C332
	community's health & safety	H63	effective	C333
	employees' health & safety	H71	forward	C411
	employees' benefits	H72	backward	C412
	employees' salaries & wages	H73	horizontal	C413
	employees' career development	H74	sources of raw materials	C421
	competitors' complying international standards	H81	distribution to final customers	C422
	competitors' quality	H82	low degree	C431
	competitors' cost	H83	medium degree	C432
	competitors' delivery	H84	high degree	C433
Competitive priorities	cost	I1	functional	C511
	quality	I2	product groups	C512
	dependability	I3	geographical	C513
	flexibility	I4	top	C521
Strategic responses	stakeholder-oriented	G1	middle	C522
	market-oriented	G2	first line	C523
	sustainability-oriented	G3	large groups	C531
Manufacturing decision categories	process technology	C1	small groups	C532
	facilities	C2	make-to-order	C611
	capacity	C3	make-to-stock	C612
	vertical integration	C4	close support	C621
	organization	C5	loose support	C622
	manufacturing planning & control	C6	high degree	C631
	quality	C7	low degree	C632
	new product introduction	C8	high quality	C711
	human resources	C9	low degree	C712
Policy areas	process choice	C11	high frequency	C721
	technology	C12	low frequency	C722
	process integration	C13	high frequency	C731
	facility size	C21	low frequency	C732
	facility location	C22	slow	C811
	facility focus	C23	fast	C812
	capacity amount	C31	standard	C821
	capacity timing	C32	customized	C822
	capacity type	C33	new processes	C831
	direction	C41	follow-the-leader- policy	C832
	extent	C42	specialized	C911
	balance	C43	not specialized	C912
	structure	C51	based on hours worked	C921
	reporting levels	C52	quantity/quality of output	C922
	support groups	C53	seniority	C923
	system design	C61	training	C931
	decision support	C62	recognition for achievement	C932
	systems integration	C63	promotion	C933
	defect prevention	C71		
	monitoring	C72		
	intervention	C73		
	rate of innovation	C81		
	product design	C82		
	industrialization	C83		
	skill level	C91		
	pay	C92		
	security	C93		

Respondents were carefully selected to provide expert judgment of the decision problem raised from this work. Initially, respondents were selected in advance and selection was based on their expertise in the manufacturing industry. This choice of respondents is consistent with the MCDM studies published by Tseng and Chiu [12]. All experts are located in the Philippines who worked for multinational manufacturing firms and were exposed to international practices. In this work, ten expert respondents were selected to provide meaningful results.

5. Results and discussion

For brevity, a sample pairwise comparisons matrix in linguistic variables from a single decision-maker is shown in Table 4.

Note that only the upper triangle of the matrix is filled out as the lower triangle represents straightforward reciprocal value of the upper triangular. This matrix describes the comparisons of stakeholders with their significance in addressing the goal of developing a sustainable manufacturing strategy. From Table 4, corresponding TFNs are shown in Table 5.

Table 4 A sample pairwise comparisons matrix in linguistic variables

	Government	Suppliers	Shareholder	Business customers	Consumers	Community	Employees	Competitors
Government		1/MO	1/MO	1/MO	1/MO	1/MO	1/MO	1/MO
Suppliers			1/MO	1/MO	1/MO	1/MO	MO	MO
Shareholders				1/MO	1/MO	MO	MO	MO
Business customers					1/MO	MO	MO	MO
Consumers						MO	MO	MO
Community							MO	MO
Employees								MO
Competitors								

Table 5 A sample pairwise comparisons matrix in TFNs

	Government	Suppliers	Shareholder	Business customers	Consumers	Community	Employees	Competitors
Government	(1,1,1)	(2/7,1/3,2/5)	(2/7,1/3,2/5)	(2/7,1/3,2/5)	(2/7,1/3,2/5)	(2/7,1/3,2/5)	(2/7,1/3,2/5)	(2/7,1/3,2/5)
Suppliers	(5/2,3,7/2)	(1,1,1)	(2/7,1/3,2/5)	(2/7,1/3,2/5)	(2/7,1/3,2/5)	(2/7,1/3,2/5)	(5/2,3,7/2)	(5/2,3,7/2)
Shareholders	(5/2,3,7/2)	(5/2,3,7/2)	(1,1,1)	(2/7,1/3,2/5)	(2/7,1/3,2/5)	(5/2,3,7/2)	(5/2,3,7/2)	(5/2,3,7/2)
Business customers	(5/2,3,7/2)	(5/2,3,7/2)	(5/2,3,7/2)	(1,1,1)	(2/7,1/3,2/5)	(5/2,3,7/2)	(5/2,3,7/2)	(5/2,3,7/2)
Consumers	(5/2,3,7/2)	(5/2,3,7/2)	(5/2,3,7/2)	(5/2,3,7/2)	(1,1,1)	(5/2,3,7/2)	(5/2,3,7/2)	(5/2,3,7/2)
Community	(5/2,3,7/2)	(5/2,3,7/2)	(2/7,1/3,2/5)	(2/7,1/3,2/5)	(2/7,1/3,2/5)	(1,1,1)	(5/2,3,7/2)	(5/2,3,7/2)
Employees	(5/2,3,7/2)	(2/7,1/3,2/5)	(2/7,1/3,2/5)	(2/7,1/3,2/5)	(2/7,1/3,2/5)	(2/7,1/3,2/5)	(1,1,1)	(5/2,3,7/2)
Competitors	(5/2,3,7/2)	(2/7,1/3,2/5)	(2/7,1/3,2/5)	(2/7,1/3,2/5)	(2/7,1/3,2/5)	(2/7,1/3,2/5)	(2/7,1/3,2/5)	(1,1,1)

Table 6 shows the corresponding crisp values of the sample pairwise comparisons matrix obtained from a single decision-maker.

From the aggregated matrix, local priority vectors, the principal eigenvalue and *CR* value were then computed. *CR* values of all pairwise comparisons matrix are below the 0.10 threshold value. The local priority vectors of all aggregated pairwise comparisons matrices are populated in the supermatrix. The general supermatrix of the decision model presented in Fig. 2 is shown in Table 7.

Table 6 A sample pairwise comparisons matrix in crisp values

	Government	Suppliers	Shareholder	Business customers	Consumers	Community	Employees	Competitors	Eigenvector
Government	1	0.3349	0.3349	0.3349	0.3349	0.3349	0.3349	0.3349	0.0398
Suppliers	2.9863	1	0.3349	0.3349	0.3349	0.3349	2.9646	2.9646	0.0902
Shareholders	2.9863	2.9863	1	0.3349	0.3349	2.9646	2.9646	2.9646	0.1557
Business customers	2.9863	2.9863	2.9863	1	0.3349	2.9646	2.9646	2.9646	0.2048
Consumers	2.9863	2.9863	2.9863	2.9863	1	2.9646	2.9646	2.9646	0.2692
Community	2.9863	2.9863	0.3373	0.3373	0.3373	1	2.9646	2.9646	0.1188
Employees	2.9863	0.3373	0.3373	0.3373	0.3373	0.3373	1	2.9646	0.0689
Competitors	2.9863	0.3373	0.3373	0.3373	0.3373	0.3373	0.3373	1	0.0525

$\lambda_{max} = 9.086, \text{C. R.} = 0.1$

Table 7 The generalized supermatrix

	A	**H#**	**H##**	**I**	**G**	**C#**	**C##**	**C###**
A	I	1	1	1	1	1	1	1
H#	H#A	I	0	H#I	0	0	0	0
H##	0	H##H#	I	0	0	0	0	0
I	IA	0	0	I	IG	0	0	0
G	GA	0	0	0	GG	0	0	0
C#	0	0	0	0	C#G	C#C#	0	0
C##	0	0	0	0	0	C##C#	I	1
C###	0	0	0	0	0	0	C###C##	I

Because the numerical supermatrix runs in the order 151×151, it is highly difficult to present it here as it requires large amount of space. For brevity, the generalized supermatrix and the resulting global priority vector are only shown to elucidate the process of the ANP. Shown in Table 8 are the decision elements with corresponding codes, the global priority vector and ranking of each element per decision component.

Table 8 Priority ranking across content of sustainable manufacturing strategy

Rank	Code	Priority policy choice	Code	Policy area
1	C711	high quality	C71	defect prevention
2	C122	flexible manufacturing system	C12	technology
3	C321	leading	C32	capacity timing
4	C812	fast	C81	rate of innovation
5	C611	make-to-order	C61	system design
6	C631	high degree	C63	systems integration
7	C821	standard	C82	product design
8	C511	functional	C51	structure
9	C831	new processes	C83	industrialization
10	C911	specialized	C91	skill level
11	C132	process	C13	process integration
12	C221	close to market	C22	facility location
13	C411	forward	C41	direction
14	C312	based on inputs	C31	capacity amount
15	C211	one big plant	C21	facility size
16	C731	high frequency	C73	intervention
17	C721	high frequency	C72	monitoring
18	C421	sources of raw materials	C42	extent
19	C621	close support	C62	decision support
20	C532	small groups	C53	support groups
21	C333	effective	C33	capacity type
22	C522	middle	C52	reporting levels
23	C112	batch	C11	process choice
24	C231	product groups	C23	facility focus
25	C432	medium degree	C43	balance
26	C931	training	C93	security
27	C922	quantity/quality of output	C92	pay

Based on Table 8, high quality defect prevention has the highest priority with respect to the goal. The 'Priority policy choice' column in Table 8 shows the content of the sustainable manufacturing strategy following stakeholders' interests. Process technology decision area is ranked first in the manufacturing strategy decision category and closely followed by capacity. Continuous consideration in material, energy and wastes flows in the production of manufacturing products highlights improvement in developing environmentally-benign technologies [38, 61]. Creation of highly energy-efficient technologies such as new machineries, new processes, new packaging, new material that produce less wastes increase the capability of manufacturing industry in supporting the triple-bottom line [62]. Process technology serves as an interesting focal point in sustainability-related advancements. In each of the manufacturing decision category, priority policy areas are: technology in process technology decision, facility location in facilities decision, capacity timing in capacity decision, direction in vertical integration decision, structure in organization decision, system design in manufacturing planning and control decision, defect prevention in quality decision, rate of innovation in new product introduction, and skill level in human resources decision. Having this prioritization enables practitioners to further focus on more important area within a decision category.

6. Conclusion

The main contribution of this work is on the development of a sustainable manufacturing strategy decision model that incorporates the interests of different stakeholders. The proposed model highlights the integration of sustainability consideration with competitive function of manufacturing. Since the model illustrates a complex decision-making under uncertainty, this paper proposed the combination of fuzzy set theory and analytic network process. Analytic network process handles the complex dependence relationships among constructs in the decision problem while fuzzy set theory addresses the uncertainty of individual judgment. Although the proposed methodological approach addresses uncertainty and vagueness in complex decision-making, performing a large number of pairwise comparisons may be cumbersome to decision-makers and may require significant amount of time. Alternatively, further simplification of the proposed decision model such that a decision hierarchy is achieved could be handled by Analytic Hierarchy Process (AHP), Technique for Order of Preference by Similarity to Ideal Solution (TOPSIS), Preference Ranking Organization Method for Enrichment Evaluation (PROMETHEE) and other multi-criteria decision-making tools. However, such simplification process may oversimplify the decision problem which may lead to counterintuitive results. Statistical tools such as structural decision modelling (SEM) could be possibly used to address the same research question but may require huge amount of data.

Nevertheless, using the proposed approach, the decision model provides the content of the sustainable manufacturing strategy. It shows that the content strategy is inclined toward process centred technology, big, product life cycle stages-focused facilities which are close to suppliers, following capacity strategy, a horizontal integration, first-line reporting with functional or geographical organizational structure, a minimal inventory-focused manufacturing planning and control, high quality prevention, monitoring and intervention policies, fast product introduction with new processes and highly skilled workers with pay based on seniority of quality/quantity of output and security focused on training or promotion. These results could guide practitioners in high level policy-making, resource allocation, strategic goal setting, process and product development, prioritization-related decision-making and in the development of programs and initiatives that address the triple-bottom line, i.e. economic, environmental and social dimensions. The content of the sustainable manufacturing strategy is expected to address both competitiveness and sustainability in manufacturing.

Acknowledgement

L. Ocampo recognizes the Ph.D. dissertation financial support from the Engineering Research and Development for Technology (ERDT) scholarship of the Department of Science and Technology, Philippines which made this work possible.

References

[1] Skinner, W. (1969). Manufacturing – missing link in corporate strategy, *Harvard Business Review*, Vol. 47, No. 3, 136-145.
[2] Wheelwright, S.C. (1984). Manufacturing strategy: Defining the missing link, *Strategic Management Journal*, Vol. 5, No. 1, 77-91, doi: 10.1002/smj.4250050106.
[3] Fine, C.H., Hax, A.C. (1985). Manufacturing strategy: A methodology and an illustration, *Interfaces*, Vol. 15, No. 6, 28-46, doi: 10.1287/inte.15.6.28.
[4] Hayes, R.H., Pisano, G.P. (1996). Manufacturing strategy: At the intersection of two paradigm shifts, *Production and Operations Management*, Vol. 5, No. 1, 25-41, doi: 10.1111/j.1937-5956.1996.tb00383.x.
[5] Paloviita, A., Luoma-aho, V. (2010). Recognizing definitive stakeholders in corporate environmental management, *Management Research Review*, Vol. 33, No. 4, 306-316, doi: 10.1108/01409171011030435.
[6] Kassinis, G., Vafeas, N. (2006). Stakeholder pressures and environmental performance, *Academy of Management Journal*, Vol. 49, No. 1, 145-159, doi: 10.5465/AMJ.2006.20785799.
[7] Baden, D.A., Harwood, I.A., Woodward, D.G. (2009). The effect of buyer pressure on suppliers in SMEs to demonstrate CSR practices: An added incentive or counter productive?, *European Management Journal*, Vol. 27, No. 6, 429-441, doi: 10.1016/j.emj.2008.10.004.
[8] Ocampo, L.A., Clark, E.E. (2014). Developing a framework for sustainable manufacturing strategies selection, *DLSU Business & Economics Review*, Vol. 23, No. 2, 115-131.
[9] Pham, D.T., Thomas, A.J. (2012). Fit manufacturing: A framework for sustainability, *Journal of Manufacturing Technology Management*, Vol. 23, No. 1, 103-123, doi: 10.1108/17410381211196311.
[10] Ocampo, L.A., Clark, E.E., Tanudtanud, K.V.G. (2015). Structural decisions of sustainable manufacturing strategy with fuzzy analytic network process (FANP), *International Journal of Strategic Decision Sciences*, Vol. 6, No. 2, 12-27, doi: 10.4018/ijsds.2015040102.
[11] Ocampo, L.A., Clark, E.E., Tanudtanud, K.V.G. (2015). A sustainable manufacturing strategy from different strategic responses under uncertainty, *Journal of Industrial Engineering*, Vol. 2015, 1-11, doi: 10.1155/2015/210568.
[12] Tseng, M.L., Chiu, A.S.F. (2013). Evaluating firm's green supply chain management in linguistic preference, *Journal of Cleaner Production*, Vol. 40, 22-31, doi: 10.1016/j.jclepro.2010.08.007.
[13] Saaty, T.L. (2001). *Decision making with dependence and feedback: The Analytic Network Process*, RWS Publications, Pittsburgh.
[14] Ocampo, L.A., Clark, E.E. (2014). A comprehensive evaluation of sustainable manufacturing programs using Analytic Network Process (ANP), *Multiple Criteria Decision Making*, Vol. 9, 101-122.
[15] Ocampo, L.A. (2015). A hierarchical framework for index computation in sustainable manufacturing, *Advances in Production Engineering & Management*, Vol. 10, No. 1, 40-50, doi: 10.14743/apem2015.1.191.
[16] Pan, R., Zhang, W., Yang, S., Xiao, Y. (2014). A state entropy model integrated with BSC and ANP for supplier evaluation and selection, *International Journal of Simulation Modelling*, Vol. 13, No. 3, 348-363, doi: 10.2507/ijsimm13(3)co13.
[17] Hayes, R.H., Wheelwright, S.C. (1984). *Restoring our competitive edge: Competing through manufacturing*, John Wiley & Sons, New York.
[18] Marucheck, A., Pannesi, R., Anderson, C. (1990). An exploratory study of the manufacturing strategy process in practice, *Journal of Operations Management*, Vol. 9, No. 1, 101-123, doi: 10.1016/0272-6963(90)90148-7.
[19] Platts, K.W., Mills, J.F., Bourne, M.C., Neely, A.D., Richards, A.H., Gregory, M.J. (1998). Testing manufacturing strategy formulation processes, *International Journal of Production Economics*, Vol. 56-57, 517-523, doi: 10.1016/S0925-5273(97)00134-5.
[20] Hallgren, M., Olhager, J. (2006). Quantification in manufacturing strategy: A methodology and illustration, *International Journal of Production Economics*, Vol. 104, No. 1, 113-124, doi: 10.1016/j.ijpe.2005.09.004.
[21] Hayes, R.H., Pisano, G.P. (1994). Beyond world-class: The new manufacturing strategy, *Harvard Business Review*, Vol. 72, No. 1, 77-86.
[22] Ward, P.T., Bickford, D.J., Leong, G.K. (1996). Configurations of manufacturing strategy, business strategy, environment and structure, *Journal of Management*, Vol. 22, No. 4, 597-626, doi: 10.1177/014920639602200404.
[23] Mani, M., Madan, J., Lee, J.H., Lyons, K., Gupta, S.K. (2012). Characterizing sustainability for manufacturing performance assessment, In: *Proceedings of the ASME 2012 International Design Engineering Technical Conferences & Computers and Information in Engineering Conference*, Chicago, Illinois, USA, 1-10.
[24] Rashid, A., Asif, F.M.A., Krajnik, P., Nicolescu, C.M. (2013). Resource conservative manufacturing: An essential change in business and technology paradigm for sustainable manufacturing, *Journal on Cleaner Production*, Vol. 57, 166-177, doi: 10.1016/j.jclepro.2013.06.012.
[25] Hassine, H., Barkallah, M., Bellacicco, A., Louati, J., Riviere, A., Haddar, M. (2015). Multi objective optimization for sustainable manufacturing, application in turning, *International Journal of Simulation Modelling*, Vol. 14, No. 1, 98-109, doi: 10.2507/ijsimm14(1)9.292.

[26] Joung, C.B., Carrell, J., Sarkar, P., Feng, S.C. (2013). Categorization of indicators for sustainable manufacturing, *Ecological Indicators*, Vol. 24, 148-157, doi: 10.1016/j.ecolind.2012.05.030.
[27] Kovac, M. (2012). Comparison of foresights in the manufacturing research, *Transfer Inovácií*, Vol. 23, 284-288.
[28] Tsai, W.H., Chou, W.C. (2009). Selecting management systems for sustainable development in SMEs: A novel hybrid model based on DEMATEL, ANP, and ZOGP, *Expert Systems with Applications*, Vol. 36, No. 2, Part 1, 1444-1458, doi: 10.1016/j.eswa.2007.11.058.
[29] Seuring, S., Müller, M. (2008). From a literature review to a conceptual framework for sustainable supply chain management, *Journal of Cleaner Production*, Vol. 16, No. 15, 1699-1710, doi: 10.1016/j.jclepro.2008.04.020.
[30] Adams, C.A., Frost, G.R. (2008). Integrating sustainability reporting into management practices, *Accounting Forum*, Vol. 32, No. 4, 288-302, doi: 10.1016/j.accfor.2008.05.002.
[31] Elkington, J. (1997). *Cannibals with forks: The triple bottom line of 21st century business*, Capstone Publishing, Oxford.
[32] Placet, M., Anderson, R., Fowler, K.M. (2005). Strategies for sustainability, *Research Technology Management*, Vol. 48, No. 5, 32-41.
[33] Baumgartner, R.J., Ebner, D. (2010). Corporate sustainability strategies: Sustainability profiles and maturity levels, *Sustainable Development*, Vol. 18, No. 2, 76-89, doi: 10.1002/sd.447.
[34] Kashmanian, R.M., Wells, R.P., Keenan, C. (2011). Corporate environmental sustainability strategy: Key elements, *Journal of Corporate Citizenship*, Vol. 2011, No. 44, 107-130, doi: 10.9774/GLEAF.4700.2011.wi.00008.
[35] Danciu, V. (2013). The sustainable company: New challenges and strategies for more sustainability, *Theoretical and Applied Economics*, Vol. 20, No. 9, 7-26.
[36] Ageron, B., Gunasekaran, A., Spalanzani, A. (2012). Sustainable supply chain management: An empirical study, *International Journal of Production Economics*, Vol. 140, No. 1, 168-182, doi: 10.1016/j.ijpe.2011.04.007.
[37] Gimenez, C., Sierra, V., Rodon, J. (2012). Sustainable operations: Their impact on the triple bottom line, *International Journal of Production Economics*, Vol. 140, No. 1, 149-159, doi: 10.1016/j.ijpe.2012.01.035.
[38] Yuan, C., Zhai, Q., Dornfeld, D. (2012). A three dimensional system approach for environmentally sustainable manufacturing, *CIRP Annals – Manufacturing Technology*, Vol. 61, No. 1, 39-42, doi: 10.1016/j.cirp.2012.03.105.
[39] De Brucker, K., Macharis, C., Verbeke, A. (2013). Multi-criteria analysis and the resolution of sustainable development dilemmas: A stakeholder management approach, *European Journal of Operational Research*, Vol. 224, No. 1, 122-131, doi: 10.1016/j.ejor.2012.02.021.
[40] Kronenberg, J., Bergier, T. (2012). Sustainable development in a transition economy: Business case studies from Poland, *Journal of Cleaner Production*, Vol. 26, 18-27, doi: 10.1016/j.jclepro.2011.12.010.
[41] Matos, S., Silvestre, B.S. (2013). Managing stakeholder relations when developing sustainable business models: The case of the Brazilian energy sector, *Journal of Cleaner Production*, Vol. 45, 61-73, doi: 10.1016/j.jclepro.2012.04.023.
[42] Griffiths, A., Petrick, J.A. (2001). Corporate architectures for sustainability, *International Journal of Operations & Production Management*, Vol. 21, No. 12, 1573-1585, doi: 10.1108/01443570110410919.
[43] Johansson, G., Winroth, M. (2010). Introducing environmental concern in manufacturing strategies: Implications for the decision criteria, *Management Research Review*, Vol. 33, No. 9, 877-899, doi: 10.1108/01409171011070305.
[44] Theyel, G., Hofmann, K. (2012). Stakeholder relations and sustainability practices of US small and medium-sized manufacturers, *Management Research Review*, Vol. 35, No. 12, 1110-1133, doi: 10.1108/01409171211281255.
[45] Perrini, F., Tencati, A. (2006). Sustainability and stakeholder management: The need for new corporate performance evaluation and reporting systems, *Business Strategy and the Environment*, Vol. 15, No. 5, 296-308, doi: 10.1002/bse.538.
[46] Clemens, B., Bakstran, L. (2010). A framework of theoretical lenses and strategic purposes to describe relationships among firm environmental strategy, financial performance, and environmental performance, *Management Research Review*, Vol. 33, No. 4, 393-405, doi: 10.1108/01409171011030480.
[47] De Brito, M.P., Carbone, V., Blanquart, C.M. (2008). Towards a sustainable fashion retail supply chain in Europe: Organization and performance, *International Journal of Production Economics*, Vol. 114, No. 2, 534-553, doi: 10.1016/j.ijpe.2007.06.012.
[48] Cheung, M.S., Myers, M.B., Mentzer, J.T. (2011). The value of relational learning in global buyer-supplier exchanges: A dyadic perspective and test of the pie-sharing premise, *Strategic Management Journal*, Vol. 32, No. 10, 1061-1082, doi: 10.1002/smj.926.
[49] Harrison, J.S., Bosse, D.A., Phillips, R.A. (2010). Managing for stakeholders, stakeholder utility functions, and competitive advantage, *Strategic Management Journal*, Vol. 31, No. 1, 58-74, doi: 10.1002/smj.801.
[50] Zadeh, L.A. (1965). Fuzzy set, *Information and Control*, Vol. 18, No. 3, 338-353, doi: 10.1016/S0019-9958(65)90241-X.
[51] Promentilla, M.A.B., Furuichi, T., Ishii, K., Tanikawa, N. (2008). A fuzzy analytic network process for multi-criteria evaluation of contaminated site remedial countermeasures, *Journal of Environmental Management*, Vol. 88, No. 3, 479-495, doi: 10.1016/j.jenvman.2007.03.013.
[52] Tseng, M.L. (2009). A causal and effect decision-making model of service quality expectation using grey-fuzzy DEMATEL approach, *Expert Systems with Applications*, Vol. 36, No. 4, 7738-7748., doi: 10.1016/j.eswa.2008.09.011.
[53] Wang, R.C., Chuu, S.J. (2004). Group decision-making using a fuzzy linguistic approach for evaluating the flexibility in a manufacturing system, *European Journal of Operational Research*, Vol. 154, No. 3, 563-572, doi: 10.1016/S0377-2217(02)00729-4.

[54] Von Altrock, C. (1996). Practical fuzzy-logic design, *The Computer Applications Journal*, Vol. 75, 1-5.
[55] Wang, C.H., Lu, I.Y., Chen, C.B. (2008). Evaluating firm technological innovation capability under uncertainty, *Technovation*, Vol. 28, No. 6, 349-363, doi: 10.1016/j.technovation.2007.10.007.
[56] Ocampo, L.A., Clark, E.E. (2014). A framework for capturing uncertainty of group decision-making in the context of the AHP/ANP, *Advances in Industrial Engineering and Management*, Vol. 3, No. 3, 7-16, doi: 10.7508/AIEM-V3-N3-7-16.
[57] Opricovic, S., Tzeng, G.H. (2003). Defuzzification within a multi-criteria decision model, *International Journal of Uncertainty, Fuzziness and Knowledge-Based Systems*, Vol. 11, No. 5, 635-652, doi: 10.1142/S0218488503002387.
[58] Tseng, M.L., Lin, Y.H., Chiu, A.S.F., Liao, J.C.H. (2008). Using FANP approach on selection of competitive priorities based on cleaner production implementation: A case study in PCB manufacturer, Taiwan, *Clean Technologies and Environmental Policy*, Vol. 10, No. 1, 17-29, doi: 10.1007/s10098-007-0109-4.
[59] Saaty, T.L. (2013). The analytic hierarchy process without the theory of Oskar Perron, *International Journal of the Analytic Hierarchy Process*, Vol. 5, No. 2, 268-293, doi: 10.13033/ijahp.v5i2.191.
[60] Saaty, T.L. (1980). *The Analytic Hierarchy Process*, McGraw-Hill, New York, USA.
[61] Smith, L., Ball, P. (2012). Steps towards sustainable manufacturing through modelling material, energy and waste flows, *International Journal of Production Economics*, Vol. 140, No. 1, 227-238, doi: 10.1016/j.ijpe.2012.01.036.
[62] Chiacchio, M.S. (2011). Early impact assessment for sustainable development of enabling technologies, *Total Quality Management and Excellence*, Vol. 39, No. 3, 1-6.

APEM journal
Advances in Production Engineering & Management
Volume 10 | Number 3 | September 2015 | pp 140–152
http://dx.doi.org/10.14743/apem2015.3.198
ISSN 1854-6250
Journal home: apem-journal.org
Original scientific paper

Effect of a milling cutter diameter on distortion due to the machining of thin wall thin floor components

Sridhar, G.[a,*], **Ramesh Babu, P.**[a]

[a]Mechanical Engineering Department, University College of Engineering, Osmania University, Hyderabad, India

ABSTRACT

Machining of prismatic blocks, removing material up to 85 % on CNC machines to produce thin wall thin floor monolithic components replacing multi part assemblies has become common in aerospace industries. The greatest challenge when machining these components is part distortion. Selecting the right kinds of tools and machining parameters is of utmost importance in minimizing distortion. One of the important parameters is the size (diameter) of the cutter. Generally, within a production scenario, the selecting the size of the cutter is driven by the productivity and geometrical constraints of the component. Experience shows that selecting the wrong size of the cutter can lead to distortion and the selecting of a correct size of the cutter depends on heuristics. In order to understand the effect of cutter diameter on distortion, machining experiments were carried out by using different sizes of milling cutter, at constant feed, speed, depth of cut and volume of material removal rate, on a representative thin wall thin floor aluminium alloy (2014A T651) component, holding the part from the bottom, using a shop made vacuum fixture. Machining simulations were also carried out to understand the machining characteristics with any change in cutter diameter at constant feed, speed, depth of cut, and material removal rate. Experimental results show that the diameter of a milling cutter has an effect on distortion at constant feed, speed, depth of cut, and volume of material removal rate.

ARTICLE INFO

Keywords:
Milling
Thin wall thin floor
Distortion
Cutter size

**Corresponding author:*
Garimella_s@yahoo.com
(Sridhar, G.)

Article history:
Received 28 December 2014
Revised 16 August 2015
Accepted 19 August 2015

1. Introduction

With recent increase in demand for more aircrafts and monolithic thin wall designs replacing complex assembles for improving performance requirements, industries are facing a great challenge in machining thin wall components [1]. Machining these components comes with many challenges to achieve required design intent. One of the many problems encountered during manufacturing of these thin wall thin floor components is machining these parts with great accuracies without distorting the part after machining. Selection of right cutting parameters along with right kind of tool to machine these thin wall thin floor components is very important [2]. Attempt made in understanding the challenges in machining these thin wall thin floor components in the previous studies [3] and survey of the literature reveal that machining fixture scheme, cutting parameters, tool geometry, design features of the component etc., [4] all play a role in effecting the final distribution of residual stresses in turn effecting the distortion of the components. Total distortion problem right from design for distortion to manufacturing processes received great attention in research field for last fifteen years [5]. It was demonstrated by Hornbach and Prevéy [6] that machining sequence plays an important role in distribution of residual stresses and optimizing the machining sequence will minimize distortion. Cui, Jung and

Moon [7] applied Taguchi method to know the effect of deformation caused by heat during cutting of aluminium alloy and found that cutting speed is the most influencing factor which causes deformation due to heat and the change of feed rate has an insignificant effect on heat deformation. Wang et al. [8] concluded that the main cause of thin walled machining distortion is due to redistribution of residual stresses during the machining process. Dong and Ke [9] verified with FEM and experiments that simulation can be done to select optimum tool path and machining sequences and avoid lengthy and expensive machining trials. Denkena and de León [10] conducted machining experiments and concluded that machining operations have influence on residual stress depth profile and showed a clear influence of residual stress distribution and part distortion on machining and tool parameters. Marusich et al. [11, 12] concluded that bulk residual stresses in the blank before machining along with the machine induced residual stresses influence distortion of the part. Bi et al. [13] proposed a simulation model taking into consideration cutting load, initial residual stresses, cutting sequence and tool path and predicted the result with an error of 19 % with experiments. Similar modelling and simulation method was proposed by Yang and Wang [14] for prediction and control of distortion. Belgasim and El-Axir [15] conducted machining experiments on aluminium magnesium alloy and observed that as per the process parameters the maximum residual stresses are either compressive or tensile, nose radius is sensitive to the residual stresses generation and feed rate is the most significant parameter affecting maximum residual stresses. Type of residual stress whether compressive or tensile depends on interfering effect of thermal and mechanical loads during machining. Izamshah et al. [16] conducted finite element analysis (FEA) and experimentation of thin walled component and proposed that FEA is an effective tool in predicting deflection and making error compensation to increase the accuracy of part eliminating expensive cutting trials. Chatelain et al. [4, 17] concluded with experiments that initial stresses embedded within the raw material has an effect on the final distortion of the component. The magnitude and distribution of the stresses effect the deformation size. Chantzis et al., [2] presented an industrial solution by first determining the initial residual stresses in the work piece, creating residual stress profiles and then optimizing the part location to minimize distortion. Songtao et al. [18] conducted machining experiment and established relationship among cutting parameters, cutting force and process deformation. They concluded that the machining deformation can be effectively controlled with combination of big radial cutting depth, small axial cutting depth at high spindle speed. Previous experimental studies conducted by authors, showed that there is significant effect of machining parameters particularly depth of cut and width of cut on distortion in machining thin wall thin floor aluminium components [19]. Huang et al. [20] conducted orthogonal experiments using high speed machining with four factors on aluminium alloy to find the residual stress distribution and concluded that decrease in cutting speed and increase in feed rate significantly increase compressive residual stresses increasing distortion. Tang et al. [21] concluded with their experiments that tool flank wear has a significant effect on residual stresses and increase in flank wear will shift from lower tensile or compressive stresses on the surface to tensile stresses. Increase in tool flank wear increases cutting forces and temperature. Xiaohui, et al. [22] concluded by conducting simulation and machining experiments that at smaller feed rate residual stresses are linearly proportional to uncut chip thickness in both tangential and radial directions and at higher feed rates only tangential residual stresses are in proportion to uncut chip thickness. They also concluded in their work to know the effect of tool diameter on residual stresses that large tool diameter will reduce uncut chip thickness and residual stress distribution is more uniform. In their experiments with 6 mm and 12 mm tools they found that maximum deformation value is reduced by 63.8 % with increase in tool diameter form 6mm to 12 mm and concluded that with further increase in diameter deformation still reduces [23]. Izamshah et al. [24] in their experimental studies on thin wall component found variation of deflection of wall with increase in helix angle of end mill.

Although some studies to understand, control and minimize machining distortion have been done by simulation and experiments, there is a lack of comprehensive study on the effect of machining distortion on machining and tool parameters which are assignable and controllable in a production shop. Hence, to study the effect of machining distortion on machining and tool pa-

rameters, attempts were made by authors in understand the challenge in machining thin wall thin floor components first [3] and carried out machining experiments to know the significance and effect of machining parameters using Taguchi experimental design [19]. It was found in a general production scenario that there is an inclination of selecting maximum size of cutter only taking geometry and accessibility into consideration, ignoring the distortion of the part caused by machining these slender thin wall thin floor components. Experience shows that machining these slender components using wrong size of cutter may distort the part. Knowing the effect of cutter size on distortion is important which will enable selection of suitable size of cutter to minimize machining distortion. So, in continuation of studies carried an attempt to understand the effect of cutter size on machining distortion keeping all machining parameters constant, a series of dry machining experiments were conducted with cutter sizes ø 6 mm to ø 16 mm which are generally used in production shops at constant material removal rate keeping all the other cutting parameters i.e., cutting speed, feed and depth of cut constant on aluminium alloy 2014A T651 used for producing avionic components, clamping the components on specially made vacuum fixture.

2. Experimental procedure

In order to find the effect of cutter size (diameter of milling cutter) on distortion of machining thin wall thin floor components, machining experiments were carried out on a representative part shown in Fig. 1.

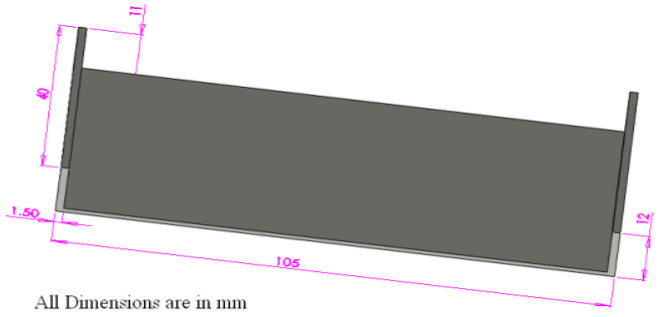

Fig. 1 Representative part used for experiments [19]

2.1 Work piece and material

The representative work piece was machined using aluminium alloy 2014 T651. This material is copper based alloy with high strength and excellent machining characteristics. The raw material was supplied as rolled plates with solution heat treatment and artificial age hardening subsequently stress relieved by stretching. This alloy is commonly used in many aerospace structural applications. The mechanical and chemical properties of the material are shown in Table 1 and Table 2 respectively. Blanks used for experiments were cut from plate with same heat number, sized to 105 mm × 40 mm × 12 mm on conventional milling machine and annealed to eliminate residual stresses within blanks.

Table 1 Mechanical properties of aluminium alloy AA2014 T651 [19]

Property	Value
Yield strength	380 MPa
Tensile strength	405 MPa
Hardness Rockwell B	82
Density	2.80 g/ cm^3
Poisson's ratio	0.2

2.2 Experimental setup

Machining experiments were carried out on 3-axis CNC vertical machining centre by holding the part from the bottom using a specially made vacuum fixture shown in Fig. 2. For consistency and to eliminate clamping effect work piece was held on the vacuum fixture as shown in Fig. 3. In total 18 random machining experiments (6 experiments with 3 replicates each) were carried by varying the diameter of milling cutter at constant cutting speed , feed per tooth, depth of cut and material removal rate. Material removal rate is calculated as given in Eq. 1, Eq. 2 and Eq. 3. Where N is Cutting speed in revolutions per minute, Vc is cutting speed in m/min, D is diameter of cutter in mm, F is feed in mm/min., Ft is feed per tooth in mm/tooth, n is number of flutes which is 2 in these experiments, DOC is depth of cut in mm, W is width of cut in mm and Q is material removal rate (MRR) in cm^3/min.

$$N = \frac{Vc \times 318.057}{D} \tag{1}$$

$$F = Ft \times n \times N \tag{2}$$

$$MRR\ (Q) = \frac{DOC \times W \times F}{1000} \tag{3}$$

Three samples were machined for each parameter and experiments were conducted randomly to reduce bias and to eliminate influence of extraneous variables during experimentation. The cutting tool path adopted for all the experiments was parallel spiral inside out as shown in Fig. 4. Width of cut is 70 % of the cutter diameter and the components were machined dry with out coolant. The cutting parameters used for experiments are shown in Table 3 and Table 4. The value of feed rate, speed and depth of cut selected were based on the available information in the factory manufacture and minimum cutter size used. The randomized experimental sequence, cutting parameters along with material removal rate is shown in Table 3.

Table 2 Chemical properties of aluminium alloy AA2014 T651 [19]

Property	Value (%)
Copper	3.8 to 4.8
Magnesium	0.2 to 0.8
Silicon	0.6 to 0.9
Iron	0.7 max
Manganese	0.2 to 1.2
Aluminium	Reminder

Fig. 2 Shop made vacuum fixture used for experiments [19]

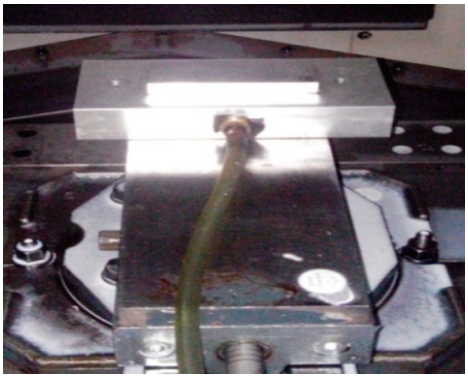

Fig. 3 Work piece held on vacuum fixture

Table 3 Machining parameters with sequence of experiments

Sl. No.	Experiment No.	Cutter size *D* (mm)	Feed *F* (mm/min)	Speed *N* (rpm)	Width of cut W (70 % of *D*) (mm)	Material removal rate *Q* (cm^3/min)
1	X22	8	955	4773	5.6	5.34
2	X31	10	764	3819	7	5.34
3	X13	6	1273	6364	4.2	5.34
4	X12	6	1273	6364	4.2	5.34
5	X61	16	478	2387	11.2	5.34
6	X23	8	955	4773	5.6	5.34
7	X51	14	546	2728	9.8	5.34
8	X42	12	637	3182	8.4	5.34
9	X33	10	764	3819	7	5.34
10	X53	14	546	2728	9.8	5.34
11	X63	16	478	2387	11.2	5.34
12	X62	16	478	2387	11.2	5.34
13	X43	12	637	3182	8.4	5.34
14	X11	6	1273	6364	4.2	5.34
15	X41	12	637	3182	8.4	5.34
16	X32	10	764	3819	7	5.34
17	X52	14	546	2728	9.8	5.34
18	X21	8	955	4773	5.6	5.34

Table 4 Cutting parameters

Parameter	Value
Feed/Tooth (*Ft*)	0.1 mm/tooth
Cutting speed (*Vc*)	120 m/min
Depth of cut (*DOC*)	1 mm
width of cut (*W*)	70 % of cutter diameter
Coolant	Dry machining

2.3 Machine tool and cutting tool

The machining experiments were carried out on Hardinge Bridgeport VMC 600 P3 3-axis vertical machining centre shown in Fig. 5 having maximum power of 13 kW and maximum spindle speed of 8000 rpm and the cutting tools used are 10 % cobalt two flute solid carbide slot drills of diameters 6 mm, 8 mm, 10 mm, 12 mm, 14 mm, and 16 mm with helix angle of 30° as shown in Fig. 6. Every experiment was carried out with new tool to avoid tool wear effect.

2.4 Distortion measurement

After conducting machining experiments, the distortion measurements were taken using Coordinate Measuring Machine (CMM), Metris LK Integra using CAMIO 4.4 software with specifications: size 800 mm × 700 mm × 600 mm, accuracy 1.9 + L/450 μm, repeatability 2.2 μm and probe error 3.6 μm. Fig. 7 shows the measurement being taken on CMM. Eighteen equally spaced similar points were marked on work piece by marking a grid as show in the Fig. 8 on opposite side to the face machined. Measurements were taken before machining on CNC and after machining and removal of work piece from the fixture on 18 similar points marked on each work piece. The difference in measurement before and after gives the distortion induced during machining [5]. Maximum deviation is taken for each work piece for distortion measurement as show in Fig. 9. The values of maximum measured distortion is given in Table 5. Apart from distortion, twist in the component after machining was also measured. Twist was measured as maximum lift in the edge of the component as shown in Fig. 10 using feeler gauge. The direction

of twist is shown in Fig. 11. Fig. 12 shows the lift produced because of twisting of the part. Maximum values of distortion and twist were used for comparison and analysis. The values of maximum measured twist is given in Table 6.

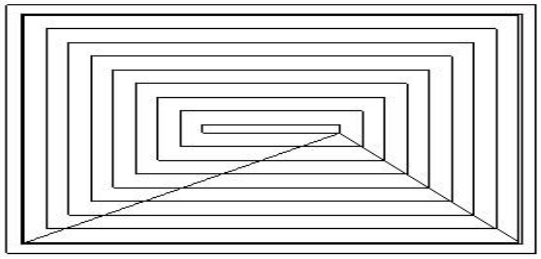

Fig. 4 Tool path layout [19]

Fig. 5 Hardinge Bridgeport VMC 600 P3

Fig. 6 Solid carbide slot drill

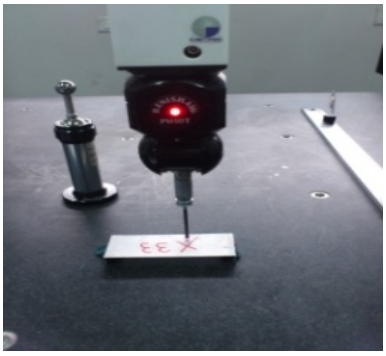

Fig. 7 CMM with work piece

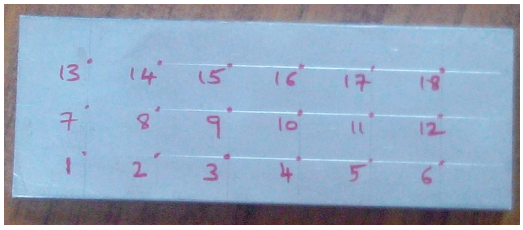

Fig. 8 Grid marking of measuring points

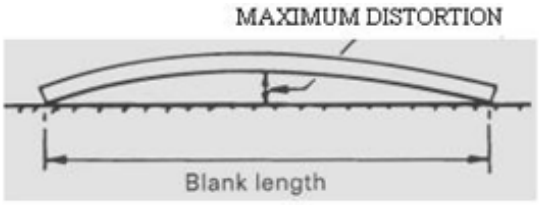

Fig. 9 Maximum distortion [19]

Table 5 Values of distortion achieved

Cutter size diameter (mm)	Distortion (mm)			
	Sample 1	Sample 2	Sample 3	Maximum
6	0.26	0.28	0.28	0.28
8	0.35	0.34	0.35	0.35
10	0.39	0.4	0.4	0.4
12	0.44	0.45	0.45	0.45
14	0.45	0.46	0.46	0.46
16	0.48	0.47	0.48	0.48

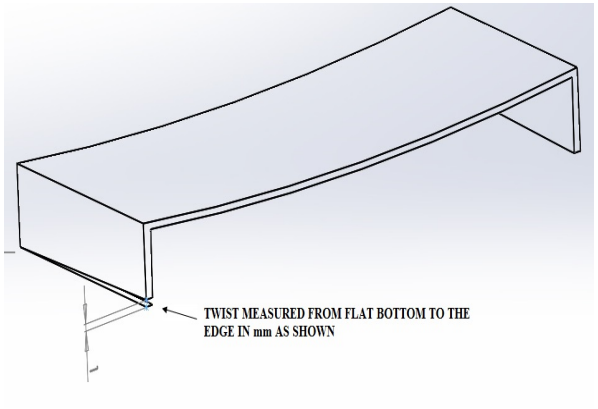

Fig. 10 Measurement of twist

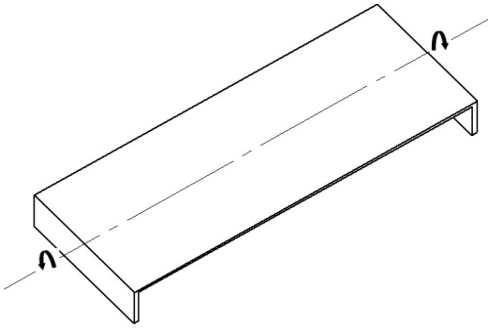

Fig. 11 Direction of twist

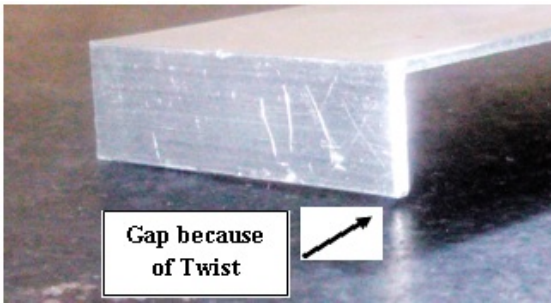

Fig. 12 Twist

Table 6 Values of twist achieved

Cutter size diameter (mm)	Twist (mm)			
	Sample 1	Sample 2	Sample 3	Maximum
6	0.29	0.3	0.3	0.3
8	0.53	0.5	0.52	0.53
10	0.78	0.8	0.77	0.8
12	0.86	0.9	0.89	0.9
14	0.98	0.99	0.97	0.99
16	1.05	1.03	1.05	1.05

2.5 FEM modelling for cutting characteristics

In order to understand the characteristics of machining aluminium alloy AA2014 T6, simulation experiments were carried at constant material removal rate, feed, speed and depth of cuts with varying milling cutter sizes, using commercial software Deform 3D. The tools and the work piece were modelled in SolidWorks and were imported to Deform 3D as .stl files. Fig. 13 shows the modelled tool. Simulations were carried using incremental Lagrangian formulation with implicit integration method. The solver used is conjugate-gradient with direct integration method. Oxley's equation to express flow stress relation is used for cutting simulation [25]. The material properties were taken from Deform 3D library. In these simulations the tool is defined rigid and is given thermal properties as it is much harder than work piece. The work piece is defined as plastic and was given both mechanical and thermal properties. Tetrahedron mesh is defined for both tool and work piece. Since milling involves high deformations at high strain rates, Deform3D uses adaptive meshing technique where in more elements are used at higher strain

rates and lesser elements at lower deformations for accuracy of solution [26]. Six runs of simulation were carried for various design of milling diameters keeping feed, speed, depth of cut and volume of material removal rate constant. In performing the simulation experiments small model of work piece is modelled for computational efficiency. Short material length of 1 mm at full width of cut defined for the cutter is chosen to save computational time without compromising the model integrity. Fig. 14 shows the milling simulation performed in Deform 3D. The instantaneous cutting force, temperature, and torque generated in simulation with stroke length are shown in Fig. 15. After simulation experiments, cutting characteristics i.e., average force in *x*, y, and *z*, average torque, average temperature and average heat flux were calculated with instantaneous simulation data for a cutter stroke of 1 mm at full width of cut. The average predicted values of cutting characteristics are given in Table 7.

Fig. 13 Modelled slot drill

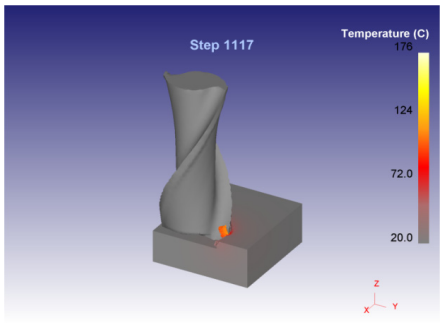

Fig. 14 FEM milling simulation using 8 mm slot drill showing transient temperature

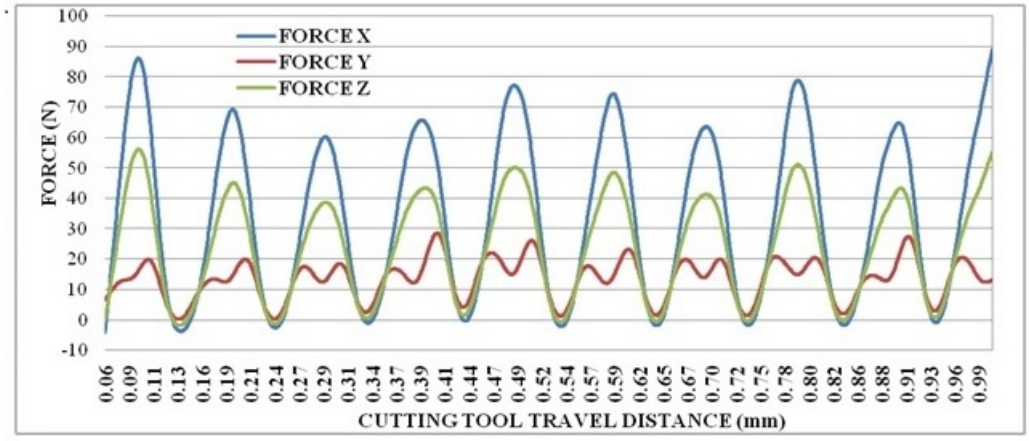

a) Cutting forces in X Y Z directions

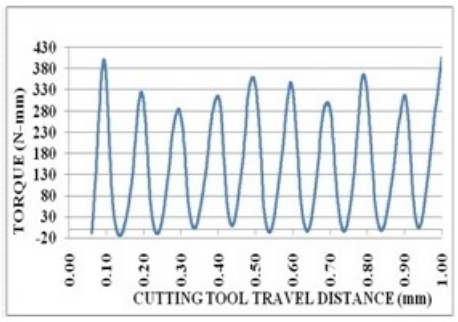

b) Torque

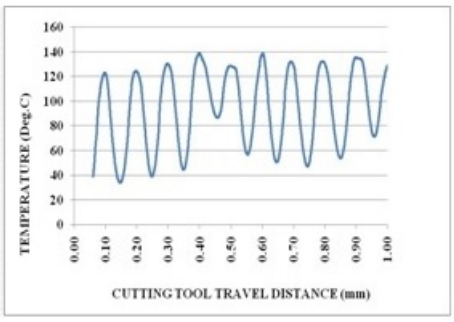

c) Temperature

Fig. 15 Instantaneous predicted: a) Cutting forces, b) Torque, and c) Temperatue generated with respect to stroke length of the cutter for 10 mm slot drill

Table 7 Simulated average predicted values of cutting characteristics

Diameter (mm)	Force (N)			Torque (N mm)	Heat flux (N mm/s)	Temperature (°C)
	X	Y	Z			
6	28.82	13.03	12.38	88.34	15033.29	92.87
8	28.13	11.19	15.62	111.94	14300.34	90.74
10	34.01	13.34	23.92	170.70	12298.63	98.62
12	32.22	13.13	27.56	195.62	10736.05	94.77
14	33.28	14.34	33.50	240.10	10536.05	102.15
16	34.01	15.02	39.33	281.51	10133.01	97.26

2.6 Chip length and chip thickness

Calculations were made to find the average chip thickness and chip length with increase in diameter of the cutter at constant feed, speed, dept of cut and material removal rates using Eq. 4 and Eq. 5 given by Martellotti [27, 28], where L_c is length of the chip in mm, D is is diameter of the cutter in mm , a_e is width of cut mm, T is number of flutes, a_f is feed per tooth in mm/tooth and a_{avg} is average chip thickness in mm. The values of average chip thickness and chip length are shown in Table 8.

$$L_c = \frac{D}{2} cos^{-1}\left(1 - \frac{2a_e}{D}\right) \pm \frac{a_f}{\pi D} T\left(\sqrt{(Da_e - a_e^2)}\right) \tag{4}$$

$$a_{avg} = \frac{a_f a_e}{L_c} \tag{5}$$

3. Results and discussion

After experiments, the effect of cutter size on distortion was evaluated by measuring the maximum distortion and twist in the components as shown in Table 5 and Table 6. To understand the cutting characteristics 6 simulation experiments were carried to evaluate average cutting forces, cutting temperature, torque and heat flux as shown in Table 7. To understand the chip characteristics, average chip length and chip thickness were calculated as shown in Table 8.

Table 8 Chip details

Diameter, D (mm)	Chip length, L_c (mm)	Average chip thickness, a_{avg} (mm)
6	5.98	0.07
8	7.96	0.07
10	9.94	0.07
12	11.92	0.07
14	13.91	0.07
16	15.89	0.07

Comparison of distortion and twist during machining is shown in Fig. 16. It could be observed from Fig. 16 and Table 5 that maximum distortion increased from 0.28 mm to 0.48 mm with increase in cutter diameter at constant feed, speed, depth of cut and material removal rate. It can also be observed from Fig. 16 and Table 6 that twist in the component increased markedly from 0.3 mm to 1.05 mm with increase in cutter diameter. Comparison of predicted cutting characteristics show marked increase in cutting forces in z-direction and torque with increase in cutter size from 6 mm to 16 mm as shown in Fig. 17 and Fig. 19, respectively. No significant increase in average cutting forces in x-direction and y-directions, and temperature as shown in Fig. 17 and

Fig. 18, respectively were noted. It is also observed that there is a slight decrease in heat flux with increase in cutter size as shown in Fig. 20. Calculations of chip length and chip thickness as in Table 8, show that, average length of chip increased with increase in cutter size and there was no change in average chip thickness.

The reason behind the increase in the deformation and twist with increase in cutter size with constant feed, speed, depth of cut and material removal rate is increase in torque and forces in *z*-direction. Further, it can be observed that there is an increase in average chip length effecting the temperature distribution indicating increase in time of contact per tooth with increase in cutter size, though there is no significant change in temperature generated during cutting. Hence, the results of experiments show that distortion of the component increase with increase in cutter diameter. So, minimum size of the cutter should be selected during machining of thin wall thin floor components to minimize distortion.

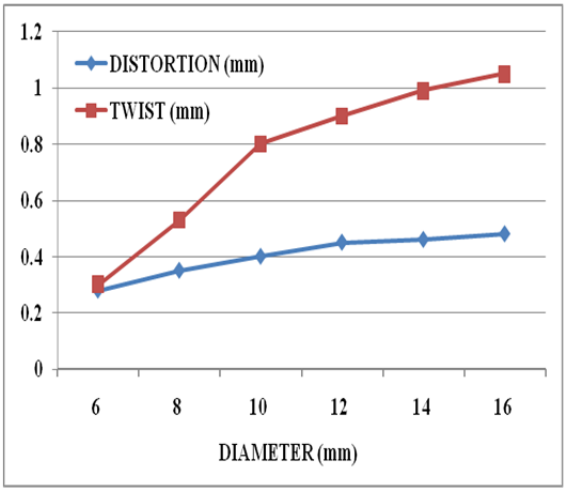

Fig.16 Distortion with change in cutter size

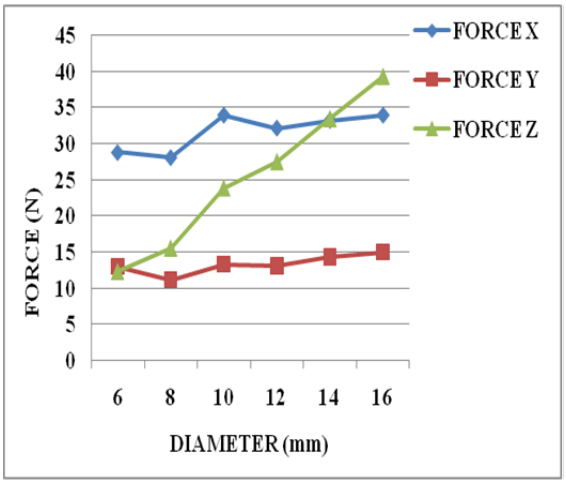

Fig. 17 Average predicted cutting forces with change in cutter size

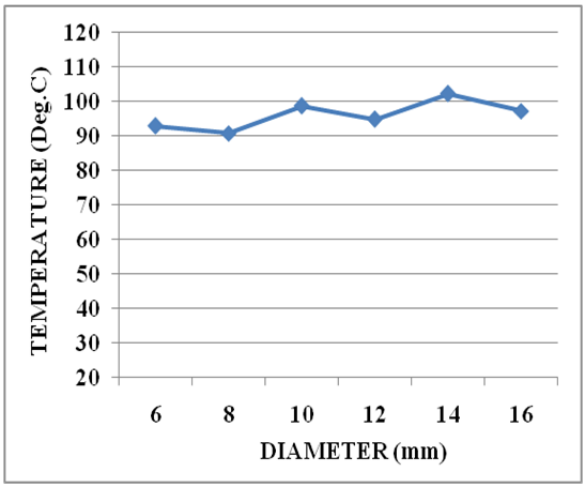

Fig. 18 Average predicted temperature with change in cutter size

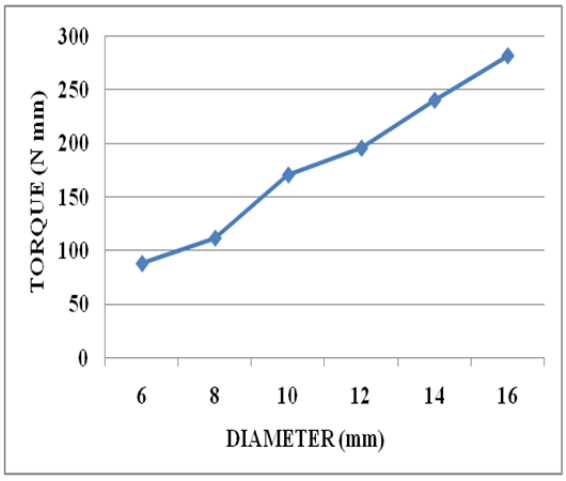

Fig. 19 Average predicted torque with change in cutter size

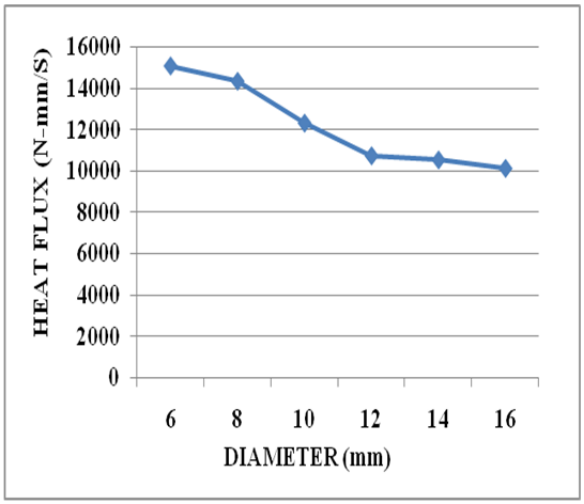

Fig. 20 Average predicted heat flux with change in cutter size

4. Conclusion

Machining experiments were conducted to know the effect of cutter size on distortion during machining. In the experimentation it is found that distortion increases with the cutter size at constant feed, speed, depth of cut and material removal rates. It is found from simulations, as the cutter size increases the forces in *z*-direction increase and play a dominant role in distorting the part and at larger cutter sizes twist in the machined part is more because of increase in cutting torque. So, precaution must be taken to see that smaller sizes of the cutter are selected for machining thin wall thin floor components to minimize distortion. Future work will focus on selection of tool geometry in terms of no. of flutes, right hand cutting, left hand cutting, helix angle and direction of helix angle and their effects on distortion.

Acknowledgement

The authors are thankful to the Head of Department, Osmania University for his constant encouragement and Support in smooth conduct of experiments. The authors are also thankful to the reviewers for their valuable inputs in enhancing the quality of the manuscript.

References

[1] Sim, W.M. (2010). Challenges of residual stress and part distortion in the civil airframe industry, *International Journal of Microstructure and Materials Properties*, Vol. 5, No. 4-5, 446-455, doi: 10.1504/IJMMP.2010.037621.

[2] Chantzis, D., Van-der-Veen, S., Zettler, J., Sim, W.M. (2013). An industrial workflow to minimise part distortion for machining of large monolithic components in aerospace industry, *Procedia CIRP*, Vol. 8, 281-286. doi: 10.1016/j.procir.2013.06.103.

[3] Sridhar, G., Babu, P.R. (2013). Understanding the challenges in machining thin walled thin floored avionics components, *International Journal of Applied Science and Engineering Research*, Vol. 2, No. 1, 93-100, doi: 10.6088/ijaser.020100010.

[4] Chatelain, J.F., Lalonde, J.F., Tahan, A.S. (2011). A comparison of the distortion of machined parts resulting from residual stresses within workpieces, In: *Proceedings of the 4th International Conference on Manufacturing Engineering, Quality and Production Systems (MEQAPS '11)*, Barcelona, Spain, 79-84.

[5] Ma, K., Goetz, R., Srivatsa, S.K. (2010). *Modeling of residual stress and machining distortion in aerospace components*, ASM Handbook, ASM.

[6] Hornbach, D., Prevéy, P. (1998). Development of machining procedures to minimize distortion during manufacture, In*: Proceedings of the 17th Heat Treating Society Conference and Exposition: Heat Treating*, ASM, Ohio, 13-18.

[7] Cui, H., Jung, J.Y., Moon, D.H. (2005). The selection of machining parameters to minimize deformation caused by heat, In: *Proceedings of the Fall Conference of Society of Korea Industrial and Systems Engineering,* Korea.

[8] Wang, Z.J., Chen, W.Y., Zhang, Y.D., Chen, Z.T., Liu, Q. (2005). Study on the machining distortion of thin-walled part caused by redistribution of residual stress, *Chinese Journal of Aeronautics*, Vol. 18, No. 2, 175-179, doi: 10.1016/S1000-9361(11)60325-7.

[9] Dong, H.Y., Ke, Y.L. (2006). Study on machining deformation of aircraft monolithic component by FEM and experiment, *Chinese Journal of Aeronautics*, Vol. 19, No. 3, 247-254, doi: 10.1016/S1000-9361(11)60352-X.

[10] Denkena, B., de León, L. (2008). Machining induced residual stress in wrought aluminium parts, In: *Proceedings of 2nd International Conference on Distortion Engineering*, Bremen, Germany, 107-114.

[11] Marusich, T.D., Stephenson, D.A., Usui, S., Lankalapalli, S. (2009). Modeling capabilities for part distortion management for machined components, from *http://www.thirdwavesys.com/*, accessed August 16, 2015.

[12] Marusich, T.D., Usui, S., Marusich, K.J. (2008). Finite element modeling of part distortion, In: Xiong, C., Liu, H., Huang, Y., Xiong, Y. (eds.), *Intelligent robotics and applications*, Lecture notes in computer science, Vol. 5315, Springer, Berlin Heidelberg, 329-338, doi: 10.1007/978-3-540-88518-4_36.

[13] Bi, Y.B., Cheng, Q.L., Dong, H.Y., Ke, Y.L. (2009). Machining distortion prediction of aerospace monolithic components, *Journal of Zhejiang University SCIENCE A*, Vol. 10, No. 5, 661-668, doi: 10.1631/jzus.A0820392.

[14] Yang, Y., Wang, Y.L. (2010). Analysis and control of machining distortion for aircraft monolithic component aided by computer, In: *Information and Computing (ICIC), 2010 Third International Conference on Information and Computing*, IEEE, Vol. 3, 280-283, doi: 10.1109/ICIC.2010.256.

[15] Belgasim, O., El-Axir, M.H. (2010). Modeling of residual stresses induced in machining aluminum magnesium alloy (Al–3Mg), In: *Proceedings of the World Congress on Engineering*, Vol. 2, London, UK, 1268-1273.

[16] Izamshah, R.A., Mo, J., Ding, S.L. (2010). Finite element analysis of machining thin-wall parts, *Key Engineering Materials*, Vol. 458, 283-288, doi: 10.4028/www.scientific.net/KEM.458.283.

[17] Chatelain, J.F., Lalonde, J.F., Tahan, A.S. (2012). Effect of residual stresses embedded within workpieces on the distortion of parts after machining, *International Journal of Mechanics*, Vol. 6, No. 1, 43-51.

[18] Songtao, W., Minli, Z., Yihang, F., Zhe, L. (2012). Cutting parameters optimization in machining thin-walled characteristics of aircraft engine architecture based on machining deformation, *Advances in Information Sciences and Service Sciences*, Vol. 4., No. 10, 244-252, doi: 10.4156/AISS.vol4.issue10.29.
[19] Sridhar, G., Ramesh Babu P. (2013). Cutting parameter optimization for minimizing machining distortion of thin wall thin floor avionic components using Taguchi technique, *International Journal of Mechanical Engineering and Technology*, Vol. 4, No. 4, 71-78.
[20] Huang, X., Sun, J., Li, J., Han, X., Xiong, Q. (2013). An experimental investigation of residual stresses in high-speed end milling 7050-T7451 aluminum alloy, *Advances in Mechanical Engineering*, Vol. 5, doi: 10.1155/2013/592659.
[21] Tang, Z.T., Liu, Z.Q., Pan, Y.Z., Wan, Y., Ai, X. (2009). The influence of tool flank wear on residual stresses induced by milling aluminum alloy, *Journal of Materials Processing Technology*, Vol. 209, No. 9, 4502-4508, doi: 10.1016/j.jmatprotec.2008.10.034.
[22] Jiang, X., Li, B., Yang, J., Zuo, X.Y., Li, K. (2013). An approach for analyzing and controlling residual stress generation during high-speed circular milling, *The International Journal of Advanced Manufacturing Technology*, Vol. 66, No. 9-12, 1439-1448. doi: 10.1007/s00170-012-4421-8.
[23] Jiang, X., Li, B., Yang, J., Zuo, X.Y. (2013). Effects of tool diameters on the residual stress and distortion induced by milling of thin-walled part, *The International Journal of Advanced Manufacturing Technology*, Vol. 68, No. 1-4, 175-186. doi: 10.1007/s00170-012-4717-8.
[24] lzamshah, R., Yuhazri, M.Y., Hadzley, M., Ali, M.A., Subramonian, S. (2013). Effects of end mill helix angle on accuracy for machining thin-rib aerospace component, *Applied Mechanics and Materials*, Vol. 315, 773-777, doi: 10.4028/www.scientific.net/AMM.315.773.
[25] Yanda, H., Ghani, J.A., Haron, C.H.C. (2010). Effect of rake angle on stress, strain and temperature on the edge of carbide cutting tool in orthogonal cutting using FEM simulation, *Journal of Engineering and Technological Sciences*, Vol. 42, No. 2, 179-194. doi: dx.doi.org/10.5614/itbj.eng.sci.2010.42.2.6.
[26] Gardner, J.D., Vijayaraghavan, A., Dornfeld, D.A. (2005). Comparative study of finite element simulation software, Laboratory for Manufacturing and Sustainability, UC Berkeley: Laboratory for Manufacturing and Sustainability, from *http://escholarship.org/uc/item/8cw4n2tf*, accessed August 16, 2015.
[27] Shaw, M.C. (2005). *Metal cutting principles*, 2nd edition, Oxford University Press, Oxford, UK.
[28] Jain, K.C., Chitale, A.K. (2010). *Textbook of production engineering*, 2nd edition, PHI Learning Pvt. Ltd., Delhi, India.

APEM journal
Advances in Production Engineering & Management
Volume 10 | Number 3 | September 2015 | pp 153–161
http://dx.doi.org/10.14743/apem2015.3.199
ISSN 1854-6250
Journal home: apem-journal.org
Original scientific paper

Experimental and simulation study on the warm deep drawing of AZ31 alloy

Reddy, A.C.S.[a,*], **Rajesham, S.**[b], **Reddy, P.R.**[c]

[a]Department of Mechanical Engineering, Narasimha Reddy Engineering College, Maisammaguda, Medchal, India
[b]Department of Mechanical Engineering, TKR college of Engineering & Technology, Hyderabad, India
[c]Department of Mechanical Engineering, CBIT, Hyderabad, India

ABSTRACT

The presented work aimed at studying the deep drawing process of a magnesium alloy sheet at elevated temperatures. This is because magnesium is being considered as a promising alternative for high strength steel and aluminium within many applications because of its low density and high specific strength. It is a well-known and recognised fact that fracturing and wrinkling during the deep drawing process can be minimised or eliminated by selecting an appropriate warm-forming temperature of the magnesium, as the formability of magnesium increases considerably as the temperature increases. Hence a warm formability study of AZ31 was performed and tested by experimental and simulation methods and resulted in superior formability at elevated temperatures in both cases. A 3D Finite element model was developed for the simulation of circular cup deep drawing and tested for different temperatures ranging from room temperature to 300 °C and it was found that the limiting drawing ratio (LDR) increased significantly with any increase in temperature. The experimental and simulation results were found to be in good agreement.

ARTICLE INFO

Keywords:
Drawing
Limiting drawing ratio (LDR)
Worm forming
Anisotropy
Forming limit diagram

**Corresponding author:*
acsreddy64@gmail.com
(Reddy, A.C.S.)

Article history:
Received 13 July 2014
First Revision 17 February 2015
Second Revision 25 March 2015
Accepted 26 March 2015

1. Introduction

It had been realized that the use of lightweight structures for aerospace, automotive and other industrial usage are vividly increased for economising the fuel consumption and minimizing the emission of hazardous gases into the atmosphere. Indeed, among the light weight metals, magnesium has gained much attention in recent years due to its light weight, i.e. 36 % lighter (by unit volume) than aluminium and 78 % lighter than iron. When magnesium is properly alloyed, attains the highest strength-to-weight ratio among all the structural metals [1]. In addition, it is having superior qualities like easy of recycling, better thermal properties, better manufacturability and close dimensional stability. As magnesium is having superior formability at higher temperatures is thus necessary to activate deformation mechanism at higher temperatures during forming process [2]. There are many significant forming parameters that are influencing of deep drawing process and they are punch nose radius, die shoulder radius, blank holder force, coefficient of friction, strain hardening exponent, strain rate sensitivity index, forming temperature and clearance between punch and die. Among these, forming temperature plays a vital role in warm forming process and needs to study the formability by means of limiting drawing ratio which is one of the formability assessment methods for deep drawing process.

Many research activities [3, 4] were aimed at investigating the improvement of the drawability and the formability of the magnesium alloy when working in warm condition. Gao En Zhi et al. [5] studied for the influence of material parameters on deep drawing of thin walled hemispheric surface part and revealed that higher punch force as n, E, σ_s increases and the influences of n and σ_s on punch force are more notable.

Warm deep drawing of magnesium alloy sheets had been performed by Ren et al. [6] using experimental method and finite element analysis. It has concluded that magnesium alloy AZ31 is sensitive to the temperature and formability is high in the temperature range 200-250 °C. Finite element simulation of deep drawing of aluminium alloy sheets at elevated temperatures by Venkateswarlu et al. [7] showed that the formability of aluminium 7075 is good in the temperature range of 150-250 °C and again from 400-500 °C.

Huang et al. [8] conducted experimental deep drawing tests on magnesium AZ31B sheets. The experimental results indicate that for 0.58 mm thinness, the highest limiting drawing ratio (LDR) is 2.63 at forming temperatures of 260 °C and for 0.50 mm thinness, highest LDR is 2.5 at 200 °C. FEM of warm forming of aluminium alloys by Kim et al. [9] was performed for forming aluminium rectangular cups at elevated temperature levels of 250 °C, 300 °C, 350 °C and observed that an increasing limiting strain with increasing forming temperature both in FEA and experiments. Forming of aluminium alloys through experimental methods by Erdin et al. [10] evaluated and concluded that as the deformation temperature increases, there is decrease in flow stress, maximum strength, hardening parameter (n), strength factor (K) but increased maximum strain. Palumbo et al. [11] did experimental analysis of worm deep drawing for Mg alloys highlighted that an improvement of LDR from 1.8 to 2.6 is feasible when adopting a draw die temperature equal to 170 °C. Deep drawing of square cups with Magnesium alloy AZ31 sheets by Chen et al. [12] revealed that both the tensile tests and forming limit tests indicate an inferior formability of AZ31 sheets at room temperature. However the formability could considerably improve when the AZ 31 sheet is stamped at elevated temperatures of 200 °C. Reddy et al. [13] demonstrated the rapid determination of LDR in order to reduce the large number of experiments and cost involved in it. The method is being well accepted by the industry in recent years. Reddy et al. [14] also conducted experiment for assessment of magnitude of the influence of different process parameters in deep drawing and concluded that blank holder force has more influence in comparison to punch nose radius and die profile radius. Patil et al. [15] conducted warm deep drawing by numerical methods and revealed that the worm temperature enhances the formability of sheet metal.

2. Yield functions

Forming of cup shaped articles by deep drawing process is actually one of the most complicated processes due to material properties such as planar anisotropy and normal anisotropy. Ideally a sheet with high normal anisotropy and zero planar anisotropy is good for deep drawing. For isotropic material r = 1 and the Von Mises yield condition can be expressed as shown in Eq. 1.

$$\bar{\sigma} = \frac{1}{\sqrt{2}}\sqrt{(\sigma_1 - \sigma_2)^2 + (\sigma_2 - \sigma_3)^2 + (\sigma_3 - \sigma_1)^2 + 6(\sigma_{12}^2 + \sigma_{23}^2 + \sigma_{31}^2)} \quad (1)$$

The anisotropic materials behaviour is more appropriately described by Hill criteria while considering the anisotropy parameters into account as described by Hill. This popular criterion described by Hill can be expressed in mathematical form as in Eq. 2.

$$\bar{\sigma} = \sqrt{\frac{F(\sigma_1-\sigma_2)^2+G(\sigma_2-\sigma_3)^2+H(\sigma_3-\sigma_1)^2+2L{\sigma_{23}}^2+2M{\sigma_{31}}^2+2N{\sigma_{13}}^2}{2}} \quad (2)$$

The F, G, H, L, M and N are constants specific to the anisotropy state of the material and 1, 2 and 3 are the principal anisotropic axes. If the tensile yield stress in the principal anisotropy directions is denoted by σ_{y1}, σ_{y2} and σ_{y3} it can be shown that

$$\left.\begin{aligned}\frac{1}{\sigma_{y1}} &= G + H \\ \frac{2}{\sigma_{y2}} &= H + F \\ \frac{3}{\sigma_{y3}} &= F + G\end{aligned}\right\} \tag{3}$$

for the ideal case of isometric materials subjected to plane stress conditions, the Mises yield criteria can be expressed as follows.

$$\sigma_f^2 = \sigma_1^2 - \sigma_1\sigma_2 + \sigma_2^2 \tag{4}$$

Similarity for material subjected to plane stress, the Hill proposed enhanced criteria for anisotropic materials while evaluating Lankford parameters in parallel and transverse to the rolling direction. The yield stress under such anisotropic conditions can be expressed as shown in Eq. 5.

$$\sigma_f^2 = \sigma_1^2 + \big((1 + r_{90})/(1 + r_0)\big)\sigma_2^2 - \big(2r_0/(1 + r_0)\big)\sigma_1\sigma_2 \tag{5}$$

If there is an effect of planar anisotropy, the quadratic Hill criterion reduces to and termed as Hasford – Backhofen equation and is as shown in Eq. 6.

$$\sigma_f^2 = \sigma_1^2 + \sigma_2^2 - \big(2r/(1 + r)\big)\sigma_1\sigma_2 \tag{6}$$

3. Determination of material properties

The Magnesium alloy AZ31 sheet had been investigated for determining the effect of temperature, anisotropy, strain hardening, strain rate sensitivity, flow stress in conjunction with evaluation of sheet metal behaviour under varying conditions. As stress-strain relations are the basic information necessitated for the study of sheet metal forming behaviour and accordingly uniaxial tensile tests were conducted while maintaining wide range of forming temperatures in concern with different strain rates. The thickness of the sheet considered were 0.9 mm and flat specimens of dog-bone shape were prepared as shown in Fig. 1 for revealing the material properties.

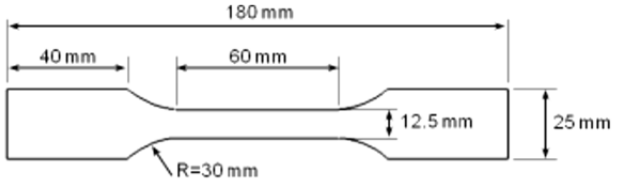

Fig. 1 Tensile test specimens used in uniaxial testing

It is also established from the literature that the AZ31 sheets exhibit anisotropic nature at lower temperatures and become isotropic over 250 °C. In order to assess anisotropic property of AZ31, samples were also prepared along 0°, 45° and 90° to the rolling direction by means of EDM cutting in order to avoid influence of edge effects due to poor cutting profile. The gauge length of 60 mm were distinguished by imprinting two marking points and was measured and recorded in order to calculate the final elongation.

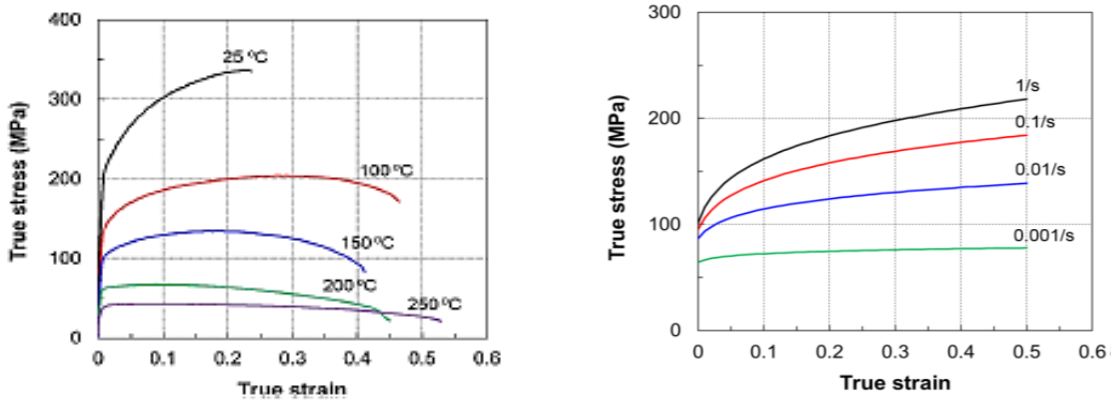

(a) (b)

Fig. 2 a) Stress-strain curves in uniaxial tension test at different temperatures; b) Effect of strain rate on the flow stress at 250 °C [16]

The tests were performed on an Instron 5582 universal testing machine with a capacity of 10 ton and a maximum crosshead speed of 500 mm/min. The tests were conducted at room temperature, 100 °C, 150 °C, 200 °C, 250 °C, 300 °C and 350 °C with the tensile axes of the test specimens aligned along the rolling direction (RD), diagonal direction (DD), and transverse direction (TD). A heating time of more than 20 min were maintained to reach the desired temperature before testing and the temperature in the chamber kept constant during each test.

The precise temperature control as well as uniform temperature distribution was maintained for accurate results. The crosshead speed of 0.06 mm/s, and strain rate of 0.001/s were applied. The variation in length, width and thickness corresponding to each load were measured for each test and ε_l, ε_w and ε_t were also evaluated. The true stress strain curves were plotted as shown in Fig. 2 and strain hardening exponent n was computed by incorporation of test results in the flow relation $\sigma = K\varepsilon^n$. The normal anisotropy can be determined with the use of expression 0.25 $(r_0 + r_{45} + r_{90})$, where r_0, r_{45}, and r_{90} orientation along 0°, 45°, and 90°, respectively.

It can be observed from Fig. 2(a) that yield stress decreases and elongation increases as the temperature increases. It is also observed that the strain hardening decreases with increase in temperature. The Fig. 2(b) illustrates the nominal stress strain relationships at 250 °C for different strain rates. It is established that higher strain rate leads to higher yield stress but reduced elongation. From the production lot, test samples were collected and upon testing observed for three types of chemical composition as shown in Table 1.

Table 1 Chemical composition of specimens (% by weight)

Specimen	Al	Zn	Mn	Fe	Ni	Mg
Type A	3.1	0.9	0.36	0.0025	0.0008	Balance
Type B	3.02	1.06	0.39	0.004	0.0005	Balance
Type C	3.09	0.83	0.38	0.0032	0.001	Balance

4. Experimental deep drawing

A preliminary experimental activity on the warm deep drawing (WDD) process of AZ31 magnesium alloy sheet was performed on 10 ton mechanical press provided with a circular tool setup consisting of axisymmetric punch, die and blank. WDD tests were performed by heating of die and while keeping the punch cool by passing cool water through the water circulation system provided in the form of passage as shown in Fig. 3.

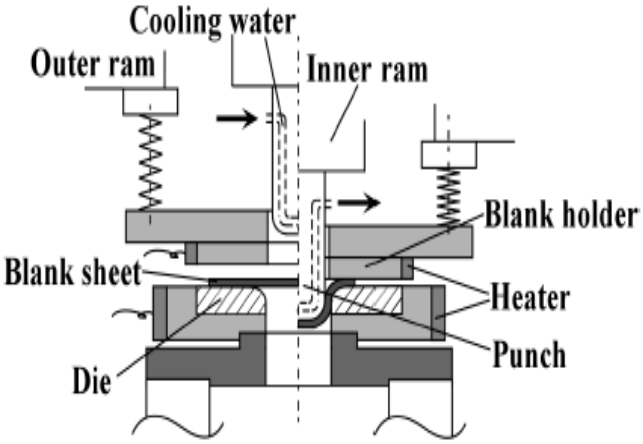

Fig. 3 Schematic representation of warm deep drawing

It shows the schematic diagram of the experimental set up used for WDD to study the forming behaviour at different temperatures. The tooling material was H13 tool steel hardened to 52 HRc. Both the die and clamp contain four 867 W electrical resistance cartridge heaters.

Embedded thermocouples were used to control the die and clamp temperature, between room temperature and 350 °C. Chilled water at a constant temperature of 10 °C was circulated through channels machined into the punch to maintain its temperature at about 14 °C. The punch temperature was also monitored using embedded thermocouple. The drawing tests were conducted for different blank sizes ranging from 150 mm to 210 mm diameter blanks with 10 mm increase in size for different worm temperatures ranging from 25 °C to 350 °C. The tool and process parameters were as depicted in Table 2.

In deep drawing test conducted at room temperature found that the induced strains in accomplishing a complete cup had crossed safe limits and hence cracks were induced as shown in Fig. 4(a). On the other hand for 300 °C temperature test of the blank observed for forming of defect free cup by maintaining all induced strains within the limiting strains as shown in Fig. 4(b).

Table 2 Tool and process parameters for experimental and simulation

Variable	Experiment	Finite element model
Blank Material	AZ31	AZ31
Blank Diameter (mm)	150 to 210 mm	150 to 210 mm
Blank Thickness (mm)	0.9	0.9
Blank Temperature (°C)	25, 100, 150, 200, 250, 300, 350	25, 100, 150, 200, 250, 300, 350
Punch Diameter (mm)	80	80
Punch nose radius (mm)	5	5
Punch temperature (°C)	25 °C	25 °C
Die opening diameter (mm)	96	96
Die Inner Diameter (mm)	83	83
Die shoulder radius (mm)	10	10
Blank holder opening diameter (mm)	96	96
Die temperature (°C)	100	100
Blank Holder force (kN)	10	10
Punch speed (mm/s)	5	5
Friction coefficient	Not reported	0.1
Contact heat transfer coefficient (W/m^2K)	Not reported	1000
Convective heat transfer coefficient (W/M^2K)	Not reported	10
Anisotropy parameters of blank	Not reported	$r_0 = 1.30$, $r_{45} = 2.5$, $r_{90} = 1.05$

a) b)

Fig. 4 a) Cups produced at room temperature, and b) cup produced at 300 °C

Experimental tests revealed that deep drawing at higher temperature gives increased formability. The LDR increased as the temperature increases and the LDR values obtained for different blank temperatures are as shown in Table 3.

Table 3 LDR for different temperatures of blank

S. No.	Temperature (°C)			LDR
	Blank	Die	Punch	
1	25	100	25	1.86
2	100	100	25	2.05
3	150	100	25	2.2
4	200	100	25	2.48
5	250	100	25	2.59
6	300	100	25	2.61
7	350	100	25	2.05

5. FEM study

Finite element analysis (FEA) technique had become a rapid and cost-effective tool for forming process and it significantly reduces the development time and cost associated with it. In essence, in-depth research has been focused on development of proper FEA models in order to accurately predict the forming behaviour and failure modes. Determination of optimal temperature for warm forming of sheet material is indeed essential requisite in order to achieve desired size, process robustness and productivity.

Experimental trial and error methods had been used in determination of appropriate temperature distribution on tooling and blank is not an easy task to achieve due to high cost, time and complexity of the process. As the complex interactions are involved among material, tooling and process, the experimental study is limited only to lab scale prototypes of industry.

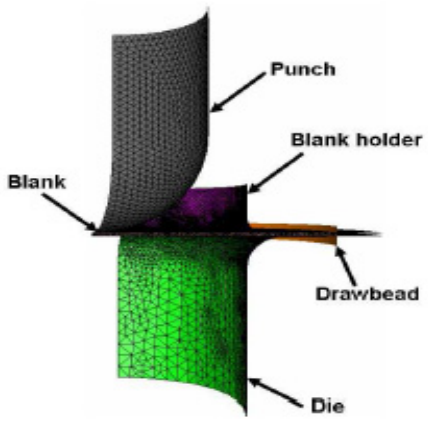

Fig. 5 Finite element mesh model for simulation

To widen the scope of warm deep drawing and to reduce product and process design lead times, essentially FEM came as an alternative in recent decades. FEM with DOE, and various optimization techniques such as artificial neural networks, genetic algorithm, multi-fidelity optimization techniques have been increasingly applied in metal forming process design and control. In this study, the worm forming of circular cup deep drawing had been analysed using commercially available FEA software ABACUS/Explicit. The tooling geometries were constructed using CAD program PRO/Engineer and were eventually converted into the finite element mesh as shown in Fig. 5.

The material properties of the AZ31 sheet obtained from the tensile tests were essentially used in the finite element simulations. The tool parameters used for simulations were die clearance of 0.6 mm on each side, blank-holder force of 2.5 kN, coefficient of friction of 0.1 and punch speed of 3 mm/s. The tooling was modelled as perfectly rigid but non-isothermal while the blank was considered as rigid visco-plastic with isotropic hardening law and following hills anisotropic yield criterion. Due to the symmetric boundary conditions and to reduce computational time, a quarter of the geometries were only modelled. The both used model have temperature and displacement as their degrees of freedom to predict both deformation and temperature variation during the process. The other input parameters for finite element simulations are as shown in Table 2.

6. Results and discussion

The formability is the ability of the sheet metal to be formed or stamped without developing any failure, and the formability increases as the temperature increases. The basic forming characteristics of sheet metals are obtained with simple tension tests. These results have been used for formulation of numerical results. The experimental result from Fig. 4 indicates that the test fails at room temperature while the cup drawn at 300 °C can be successfully dawn without any defects. The LDR increased gradually as the deep drawing temperature increases in warm forming the LDR starts decreases after 300 °C as shown in Table 3.

The finite element tests have been conducted for the 150 mm blank diameter using FEA software ABACUS/Explicit. The deep drawn cups are produced without any incipient necking or fracture and the LDR in considerably high at the temperature of 300 °C.

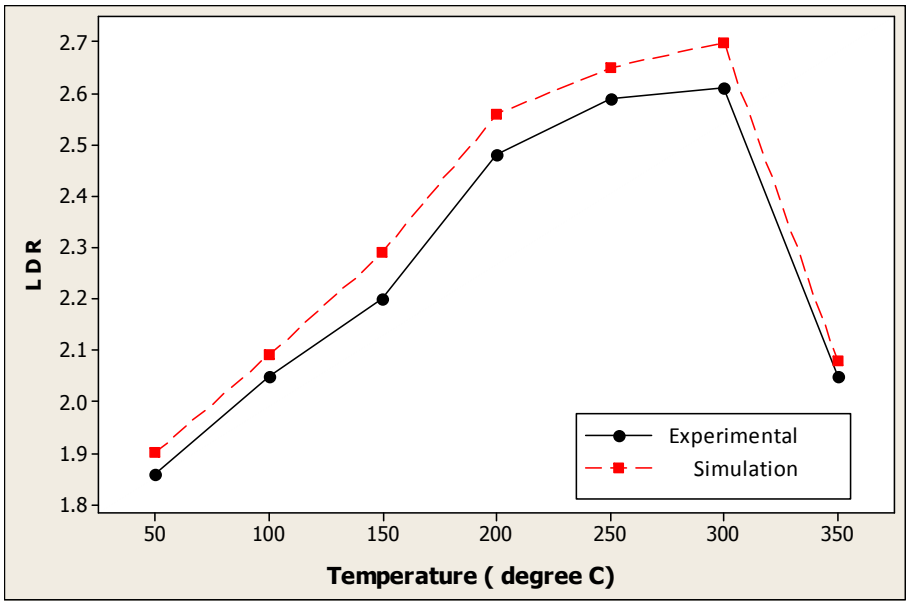

Fig. 6 LDR for experimental and simulation for different temperatures of the blank

The Fig. 6 shows the comparison of the experimental and simulated results and found that LDR increased significantly as the temperature increases from ambient temperature to 300 °C in both experimental and simulation results. The reason for poor formability above 300 °C is due to the tendency of sheet for localised necking and limits the formability in deep drawing of cups especially at the regions very close to punch nose radius. Once this instability occurs, the load carrying capacity decreases gradually due to decrease in thickness of the material and hence reduced LDR. The onset of localized necking needs to be predicted accurately in order to determine the forming limits of the material. It have be observed that the LDR can be significantly achieved about 2.6 at 300 °C and hence warm forming can be successfully used for deep drawing at elevated temperatures. In addition to that the amount of blank holder force required also decreases due to decreased flow stress at higher temperatures.

It can be observed from simulation results that the LDR obtained from simulation are slightly higher than that of the experimental results. This might be due to the complexity involved in the finite element models in selecting an appropriate and correct model for simulation results. The accuracy of FE simulation results are highly dependent on the type yielding and temperature dependent flow stress models used in describing the flow properties of the material.

7. Conclusion

In this study, formability of AZ31 studied both experimentally and numerically using FEM software ABAQUS. In both cases LDR increased significantly as the temperature increases. The deep drawing tests were conducted at 25 °C, 100 °C, 150 °C, 200 °C, 250 °C, 300 °C and 350 °C. Hence proper temperature selection is very essential for deep drawing of AZ31 cups without incipient necking and cracks.

Acknowledgements

The corresponding author would like to thank the Holy Mary Institute of Technology, Hyderabad for allowing use the Laboratory facilities available in the institute. The author is also thankful to Dr. B.S. Verma, Principal, HITS, Hyderabad for his continuous inspiration in doing research.

References

[1] Bieler, T.R., Mishra, R.S., Mukherjee, A.K. (1996). Superplasticity in hard-to-machine materials, *Annual Review of Materials Science*, Vol. 26, 75-106, doi: 10.1146/annurev.ms.26.080196.000451.

[2] Nguyen, N.T., Seo, O.S., Lee, C.A., Lee, M.G., Kim, J.H., Kim, H.Y. (2014). Mechanical behavior of AZ31B Mg alloy sheets under monotonic and cyclic loadings at room and moderately elevated temperatures, *Materials*, Vol. 7, No. 2, 1271-1295, doi: 10.3390/ma7021271.

[3] Lee, J.D., Heo, Y.M., Chang, S.H., Choi, Y.C., Kim, H.Y., Seo, D.G. (2001). A study on the warm deep drawability of sheets in Cr-coated die, *KSME International Journal*, Vol. 15, No. 7, 839-846.

[4] Venkateswarlu, G., Davidson, M.J., Tagore, G.R.N., (2010). Influence of process parameters on the cup drawing of aluminum 7075 sheet, *International Journal of Engineering, Science and Technology,* Vol. 2, No. 11, 41-49, doi: 10.4314/ijest.v2i11.64553.

[5] Gao, E.Z., Li, H.W., Kou, H.C., Chang, H., Li, J.S., Zhou, L. (2009). Influence of material parameters on deep drawing of thin-walled hemispheric surface part, *Transactions of Nonferrous Metals Society of China*, Vol. 19, No. 2, 433-437, doi: 10.1016/S1003-6326(08)60291-5.

[6] Ren, L.M., Zhang, S.H., Palumbo, G., Tricarico, L. (2008). Warm deep drawing of mfgnesium alloy sheets – Formability and process conditions, *Proceedings of the Institution of Mechanical Engineering, Part B: Journal of Engineering Manufacture,* Vol. 222, No. 11, 1347-1354, doi: 10.1243/09544054JEM1114.

[7] Venkateswarlu, G., Davidson, M.J., Tagore, G.R.N. (2010). Finite element simulation of deep drawing of aluminum alloy at elevated temperatures, *ARPN Journal of Engineering and Applied Sciences*, Vol. 5, No. 7, 93-98.

[8] Huang, T.B., Tsai, Y.A., Chen, F.K. (2006). Finite element analysis and formability of non-isothermal deep drawing of AZ31B sheets, *Journal of Material Processing Technology*, Vol. 177, No. 1-3, 142-145, doi: 10.1016/j.jmatprotec.2006.04.088.

[9] Kim, H.S., Koç, M., Ni, J., Ghosh, A. (2006). Finite element modelling and analysis of warm forming of aluminum alloys – Validation through comparisons with experiments and determination of a failure criterion, *Journal of Manufacturing Science and Engineering,* Vol. 128, No. 3, 613-621, doi: 10.1115/1.2194065.

[10] Erdin, M.E., Aykul, H., Tunalıoğlu, M.Ş. (2005). Forming of high strength/low formability metal sheets at elevated temperatures, *Mathematical and Computational Applications*, Vol. 10, No. 3, 331-340.
[11] Palumbo, G., Sorgente, D., Tricarico, L., Zhang, S.H., Zheng, W.T. (2006). Numerical and experimental analysis of the warm deep drawing process for Mg alloys, *Journal of Achievements in Materials and Manufacturing Engineering,* Vol. 14, No. 1-2, 111-118.
[12] Chen, F.K., Huang, T.B., Chang, C.K. (2003). Deep drawing of square cups with magnesium alloy AZ31 sheets, *International Journal of Machine Tools and Manufacture*, Vol. 43, No. 15, 1553-1559, doi: 10.1016/S0890-6955(03)00198-6.
[13] Reddy, A.C.S., Rajesham, S., Reddy, P.R. (2014). Evaluation of limiting draing ratio (LDR) in deep drawing by rapid determination method, *Internal Journal of Current Engineering and Technology,* Vol. 4, No. 2, 757-762.
[14] Reddy, A.C.S., Rajesham, S., Reddy, P.R., Kumar, T.P., Goverdhan, J. (2015). An experimental study on effect of process parameters in deep drawing using Taguchi technique, *International Journal of Engineering, Science and Technology.* Vol. 7, No. 1, 21-32, doi: 10.4314/ijest.v7i1.3.
[15] Patil, S.M., Hussain, S.M., Kumar, K.R. (2014). Experimental and numerical analysis of springback in deep drawing process, *Global Journal of Engineering Science and Researches,* Vol. 1, No. 7, 2014, 15-24.
[16] Liu, Z. (2012). *Numerical and experimental study of AZ31-O magnesium alloy warm sheet forming,* Doctoral dissertation, Ecole Nationale Supérieure des Mines de Paris, from *https://pastel.archives-ouvertes.fr/pastel-00718370/document*, accessed March 25, 2015.

Calendar of events

- 17th International Conference on Emerging Trends in Engineering and Technology, Geneva, Switzerland, September 7-8, 2015.
- IEEE 20th Conference on Emerging Technologies & Factory Automation, Luxembourg, Luxembourg, September 8-11, 2015.
- ICMSE 2015: International Conference on Manufacturing Science and Engineering, Berlin, Germany, September 14-15, 2015.
- 23rd International Conference on Materials and Technology, Portorož, Slovenia, September 27-30, 2015.
- IEEE/RSJ International Conference on Intelligent Robots and Systems (IROS 2015), Hamburg, Germany, September 28 – October 2, 2015.
- The 56th Conference on Simulation and Modelling, Linköping, Sweden, October 7-9, 2015.
- 26th DAAAM International Symposium 2015, Zadar, Croatia, October 21-24, 2015.
- 16th International Manufacturing Conference in China, Hangzhou, China, October 22-25, 2015.
- 17th International Conference on Engineering Systems Modeling, Simulation and Analysis, Paris, France, October 29-30, 2015.
- 17th International Conference on Advanced Mechanical and Manufacturing Design Technology, Venice, Italy, November 9-10, 2015.
- 5th International Conference on Accuracy in Forming Technology ICAFT 2015, Chemnitz, Germany, November 10-11, 2015.
- ASME – International Mechanical Engineering Congress & Exposition (IMECE), Houston, Texas, United States, November 13-19, 2015.
- 17th International Conference on Supply Chain and Logistics Management, Dubai, UAE, November 24-25, 2015.
- 17th International Conference on Automotive Engineering and Intelligent Manufacturing, Bangkok, Thailand, December 17-18, 2015.
- 18th International Conference on Numerical Methods in Industrial Processes, Paris, France, January 21-22, 2016.
- 18th International Conference on Mechatronics and Intelligent Manufacturing, Istanbul, Turkey, January 25-26, 2016.
- 6th CIRP Conference on Assembly Technologies and Systems, Gothenburg, Sweden, May 16-17, 2016.
- 49th CIRP Conference on Manufacturing Systems, Stuttgart, Germany, May 25-27, 2016.
- 3rd CIRP Conference on Surface Integrity, Charlotte, NC, USA, June 8-10, 2016.
- 10th CIRP Conference on Intelligent Computation in Manufacturing Engineering, Gulf of Naples, Italy, July 20-22, 2016.
- International Conference on Design and Production Engineering, Berlin, Germany, July 25-26, 2016.

Notes for contributors

General

Articles submitted to the *APEM journal* should be original and unpublished contributions and should not be under consideration for any other publication at the same time. Extended versions of articles presented at conferences may also be submitted for possible publication. Manuscript should be written in English. Responsibility for the contents of the paper rests upon the authors and not upon the editors or the publisher. Authors of submitted papers automatically accept a copyright transfer to *Production Engineering Institute*, *University of Maribor*.

Submission of papers

A submission must include the corresponding author's complete name, affiliation, address, phone and fax numbers, and e-mail address. All papers for consideration by *Advances in Production Engineering & Management* should be submitted by e-mail to the journal Editor-in-Chief:

Miran Brezocnik, Editor-in-Chief
UNIVERSITY OF MARIBOR
Faculty of Mechanical Engineering
Production Engineering Institute
Smetanova ulica 17, SI – 2000 Maribor
Slovenia, European Union
E-mail: editor@apem-journal.org

Manuscript preparation

Manuscript should be prepared in *Microsoft Word 2007* (or higher version) word processor. *Word .docx* format is required. Papers on A4 format, single-spaced, typed in one column, using body text font size of 11 pt, should have between 8 and 12 pages, including abstract, keywords, body text, figures, tables, acknowledgements (if any), references, and appendices (if any). The title of the paper, authors' names, affiliations and headings of the body text should be in *Calibri* font. Body text, figures and tables captions have to be written in *Cambria* font. Mathematical equations and expressions must be set in *Microsoft Word Equation Editor* and written in *Cambria Math* font. For detail instructions on manuscript preparation please see instruction for authors in the *APEM journal* homepage *apem-journal.org*.

The review process

Every manuscript submitted for possible publication in the *APEM journal* is first briefly reviewed by the editor for general suitability for the journal. Notification of successful submission is sent. After initial screening the manuscript is passed on to at least two referees. A double-blind peer review process ensures the content's validity and relevance. Optionally, authors are invited to suggest up to three well-respected experts in the field discussed in the article who might act as reviewers. The review process can take up to eight weeks. Based on the comments of the referees, the editor will take a decision about the paper. The following decisions can be made: accepting the paper, reconsidering the paper after changes, or rejecting the paper. Accepted papers may not be offered elsewhere for publication. The editor may, in some circumstances, vary this process at his discretion.

Proofs

Proofs will be sent to the corresponding author and should be returned within 3 days of receipt. Corrections should be restricted to typesetting errors and minor changes.

Offprints

An e-offprint, i.e., a PDF version of the published article, will be sent by e-mail to the corresponding author. Additionally, one complete copy of the journal will be sent free of charge to the corresponding author of the published article.

APEM journal

Advances in Production Engineering & Management

Production Engineering Institute (PEI)
University of Maribor
APEM homepage: apem-journal.org

Volume 10 | Number 3 | September 2015 | pp 111-164

Contents

Scope and topics 114

Characterizations of 304 stainless steel laser cladded with titanium carbide particles 115
Mahmoud, E.R.I.

An integrated sustainable manufacturing strategy framework using fuzzy analytic network process 125
Ocampo, L.A.; Clark, E.E.; Tanudtanud, K.V.G.; Ocampo, C.O.V.; Impas Sr., C.G.; Vergara, V.G.; Pastoril, J.; Tordillo, J.A.S.

Effect of a milling cutter diameter on distortion due to the machining of thin wall thin floor components 140
Sridhar, G.; Ramesh Babu, P.

Experimental and simulation study on the warm deep drawing of AZ31 alloy 153
Reddy, A.C.S.; Rajesham, S.; Reddy, P.R.

Calendar of events 162

Notes for contributors 163

ISSN 1854-6250

apem-journal.org